The CORDEX Flagship Pilot Study in Southeastern South America: A comparative study of statistical and dynamical downscaling models in simulating daily extreme precipitation events

Bettolli ML[1,2*], Solman SA[1,2,3], da Rocha RP[4], Llopart M[5], Gutierrez JM[6], Fernández J[7], Olmo ME[1,2], Lavin-Gullon A[6], Chou SC[8], Carneiro Rodrigues D[9], Coppola E[10], Balmaceda Huarte R[1,2], Barreiro M[11], Blázquez J[2,3,12], Doyle M[1,2,3], Feijoó M[2,3], Huth R[13], Machado L[9], Vianna Cuadra S[14]

*Corresponding author. E-mail address: bettolli@at.fcen.uba.ar

Affiliations

[1]Department of Atmospheric and Ocean Sciences, Faculty of Exact and Natural Sciences, University of Buenos Aires (DCAO-FCEN-UBA) and National Council of Scientific and Technical Research (CONICET), Buenos Aires, Argentina

[2]Institut Franco- Argentin d'Estudes sur le Climat et ses Impacts, Unité Mixte Internationale (UMI-IFAECI/CNRS-CONICET-UBA), Buenos Aires, Argentina

[3]Centro de Investigaciones del Mar y la Atmósfera (CIMA), CONICET-UBA, Buenos Aires, Argentina

[4]Departamento de Ciências Atmosféricas, Universidade de São Paulo (USP), São Paulo, SP, Brazil

[5]Universidade Estadual Paulista Júlio de Mesquita Filho (UNESP) and Centro de Meteorologia de Bauru (IPMet), Bauru, SP, Brazil

[6]Meteorology Group, Instituto de Física de Cantabria (IFCA), CSIC-Univ. Cantabria, Santander, Spain

[7]Meteorology Group, Department of Applied Mathematics and Computer Science, Universidad de Cantabria, Santander, Spain

[8]Centro de Previsão de Tempo e Estudos Climáticos - INPE, São Paulo, SP, Brazil

[9]Instituto Nacional de Pesquisas Espaciais (INPE), São José dos Campos, SP, Brazil

[10]International Centre for Theoretical Physics (International Center for Theoretical Physics (ICTP)), Trieste, Italy

[11]Departamento de Ciencias de la Atmósfera, Facultad de Ciencias, Universidad de la República, Montevideo, Uruguay

[12]Facultad de Ciencias Astronómicas y Geofísicas, Universidad Nacional de La Plata, La Plata, Argentina

[13]Department of Climatology, Institute of Atmospheric Physics, Academy of Sciences of the Czech Republic and Department of Physical Geography and Geoecology, Faculty of Science, Charles University, Prague, Czech Republic

[14]Brazilian Agricultural Research Corporation (EMBRAPA), Brasília, DF, Brazil

0000-0002-7750-2979 Llopart

0000-0001-7423-0544 Bettolli

0000-0001-6693-9393 Solman

0000-0003-3378-393X Porfirio da Rocha

0000-0002-2766-6297 Gutiérrez

0000-0003-0858-8999 Doyle

0000-0002-3483-0008 Fernandez

0000-0003-3276-012X Blázquez

0000-0003-1665-1337 Lavin-Gullon

0000-0002-7819-1607 Barreiro

Acknowledgments

Thanks to CORDEX for endorsing the FPS-SESA. This work was supported by the University of Buenos Aires 2018-20020170100117BA grant; JMG, MLB, SAS, RPR funding from the Spanish Research Council (CSIC) I-COOP+ Program "reference COOPB20374". JMG, JF and AL-G acknowledge support from the Spanish R&D Program through projects MULTI-SDM (CGL2015-66583-R) and INSIGNIA (CGL2016-79210-R), co-funded by the European Regional Development Fund (ERDF/FEDER). AL-G acknowledges support from the Spanish R&D Program through the predoctoral contract BES-2016-078158. Universidad de Cantabria simulations have been carried out on the Altamira Supercomputer at the Instituto de Física de Cantabria (IFCA-CSIC), member of the Spanish Supercomputing Network. MB acknowledges support from the Simons Associateship of the Abdus Salam International Centre for Theoretical Physics. RH acknowledges support from the project LTT17007 funded by the Ministry of Education, Youth, and Sports of the Czech Republic.

ABSTRACT

The aim of this work is to present preliminary results of the statistical and dynamical simulations carried out within the framework of the Flagship Pilot Study in southeastern South America (FPS-SESA) endorsed by the Coordinated Regional Climate Downscaling Experiments (CORDEX) program. The FPS-SESA initiative seeks to promote inter-institutional collaboration and further networking with focus on extreme rainfall events. The main scientific aim is to study multi-scale processes and interactions most conducive to extreme precipitation events through both statistical and dynamical downscaling techniques, including convection-permitting simulations. To this end, a targeted experiment was designed considering the season October 2009 to March 2010, a period with a record number of extreme precipitation events within SESA. Also, three individual extreme events within that season were chosen as case studies for analyzing specific regional processes and sensitivity to resolutions. Four dynamical and four statistical downscaling models (RCM and ESD respectively) from different institutions contributed to the experiment. In this work, an analysis of the capability of the set of the FPS-SESA downscaling methods in simulating daily precipitation during the selected warm season is presented together with an integrated assessment of multiple sources of observations and available CORDEX Regional Climate Model simulations. Comparisons among all simulations reveal that there is no single model that performs best in all aspects evaluated. The ability in reproducing the different features of daily precipitation depends on the model. However, the evaluation of the sequence of precipitation events, their intensity and timing suggests that FPS-SESA simulations based on both RCM and ESD yield promising results. Most models capture the extreme events selected, although with a considerable spread in accumulated values and the location of heavy precipitation.

Keywords: Extreme precipitation; Statistical and Dynamical Downscaling; Observational Uncertainty, Southeastern South America

1. INTRODUCTION

Southeastern South America (SESA) covers central-northeastern Argentina, Uruguay and the southern portions of Brazil and Paraguay (roughly between 20–40° S, 45–65° W, Fig. 1 (a)). It is a highly populated region with large urban settlements. The socio-economic activities are mainly based on rainfed agriculture production and cattle raising,

for both domestic consumption and exports. Rivers in SESA provide hydroelectric power utilities, which supply energy to the region and water for consumption, while navigation along them facilitates the integration of regional economies (Barros et al. 2006).

The precipitation regime in SESA shows a uniform seasonal cycle with large amounts of precipitation throughout the year, frequently associated with extreme precipitation events, which are the main contributors to the hydrologic cycle in SESA. They are associated with extratropical synoptic activity during the cold season, cyclogenesis particularly during transition seasons, and mesoscale convective systems during the warm season (October to May) (Cavalcanti 2012; Durkee et al. 2009). These complex convective systems account for large fractions (60-80%) of the annual total precipitation amounts (Nesbitt et al. 2006); hence, extreme precipitation events are of special importance to the region, particularly during the warm season. Although these events contribute positively by providing significant water volumes to recharge soil moisture and rivers, they are frequently associated with intense rainfall and hail, causing severe direct damages to population and farm lots.

Diverse forcings in different temporal and spatial scales influence precipitation extremes in SESA. The low-level jet east of the Andes plays a vital role for the availability of heat and moisture from low latitudes, that in combination with the upper level subtropical jet, the presence of a thermal low pressure center in northwestern Argentina and a lee trough at upper levels of the atmosphere provide the favorable instability background for the development of convective systems (Saulo et al. 2004; Salio et al. 2007; Teixeira and Satyamurty 2007; Rozante and Cavalcanti 2008; Durkee et al. 2009, Ungerovich and Barreiro 2019). The Andes range orographic barrier acts not only as a channel, favoring meridional exchange of air masses (Seluchi and Marengo 2000), but also as a topographical influence on the initiation and maintenance of convective systems (Rasmussen and Houze 2016). Additionally, local processes and remote forcings such as ENSO, local air–sea coupling in the south Atlantic Ocean and the South Atlantic Convergence Zone exert a strong influence in the intensity, frequency and position of these extreme events (Doyle and Barros 2002; Boulanger et al. 2005; Barreiro 2010).

Studies devoted to evaluating the capability of Global Climate Models (GCMs) in simulating the daily precipitation over SESA showed that they exhibit difficulties in representing the correct combination of frequency and intensity of precipitation, particularly for extreme events (Bettolli and Penalba 2014; Asadieh and Krakauer 2015). By design, GCMs are not able to simulate regional climate characteristics (Maraun et al. 2010, Barros and Doyle 2018). Therefore, the complexity of the processes, forcings and interactions involved in the precipitation extremes over SESA is weakly captured. Regional climate models (RCMs), using GCMs as boundary conditions, simulate climate processes with finer spatial resolution than GCMs and, in consequence, yield a better representation of processes leading to precipitation events (Rummukainen 2010). Different evaluations of RCMs operating at horizontal resolutions in the range from 20 to 50 km have demonstrated the added value of the increased resolution to simulate the precipitation intensity distributions over SESA (da Rocha et al. 2009; Giorgi et al. 2014; Llopart et al. 2014; Reboita et al. 2016; Mourão et al. 2015; Falco et al. 2019; Solman and Blázquez 2019). However, convection-permitting RCM simulations, running at horizontal grid spacings of a few kilometers, have been shown to better capture precipitation extremes in other regions of the world (Prein et al. 2015; Scaff et al. 2019; Coppola et al. 2019) and have not been explored over SESA yet. These studies agree that the use of convection-permitting RCM improves the representation of the diurnal cycle of convective precipitation during the summer months, the intensity of extreme precipitation events associated with deep convection and convective precipitation forced by orography.

Another approach to resolve the scale discrepancy between GCMs coarse simulations and local scales is the empirical statistical downscaling (ESD), that establishes empirical/statistical relationships between large-scale atmospheric variables and local climate (Maraun et al. 2010). Unlike other parts of the world, the ESD community is emergent and still small in the region. Thus, limited studies analyzing the ESD potential to simulate daily precipitation and extremes in SESA are available. However, probabilistic estimates of daily precipitation based on the k-means technique and the self-organizing maps (D'onofrio et al. 2010) as well as deterministic simulations based on the analog method (Bettolli and Penalba 2018) gave evidence of the potential of the ESD models in representing different properties of daily precipitation over the region such as mean values, day-to-day variance, daily correspondence, persistence, inter-annual variability, probability distributions and extreme percentiles.

Comparative evaluations of RCM and ESD simulations suggest that both approaches show similar skills to represent regional climate characteristics (Haylock et al. 2006; Menéndez et al. 2010; Huth et al. 2015; Casanueva et al. 2019), though with different strengths and weaknesses (Fowler et al. 2007). Performance of downscaling approaches may vary from one region to another depending on the local conditions, as well as the climate variable of interest. Hence, the importance of developing RCM and ESD coordinated actions relies on the fact that combining different models and approaches, different processes and sources of uncertainties can be assessed when addressing the study of a specific regional climate phenomenon. Up to now, the study conducted by Menendez et al. (2010) was the only coordinated exercise carried out in SESA to study extreme precipitation anomalies as simulated by one stretched-grid atmospheric global model, five different RCM and one statistical downscaling technique. The authors found that most of the dynamical models underpredicted precipitation amounts. However, the model ensemble and the statistical technique succeeded in reproducing the overall observed frequency of daily precipitation, though underestimating the frequency of heavy precipitation events. Recommendations on further research to understand the models' capabilities and the variety of simulated feedbacks in the region, as well as to explore the combination of different downscaling sources emerged from this exercise.

All of the above aligns with several scientific challenges recognized by the Scientific Advisory Team of the Coordinated Regional Climate Downscaling Experiment (CORDEX) of the Word Climate Research Programme (WCRP) to set up targeted experiments called Flagship Pilot Studies (FPS). The scientific challenges identified are the need for: 1) more rigorous and quantitative assessment of the added value of regional downscaling; 2) better understanding of processes and phenomena relevant for regional climate change; 3) better integration of ESD within the CORDEX framework; 4) moving towards very high resolution models, reaching convection permitting horizontal resolutions; 5) distillation of actionable information from multiple sources of downscaled projection information. In this context, the FPS in southeastern South America (FPS-SESA) focuses on extreme precipitation events, their modelling, understanding and impacts addressing these scientific tasks. The objectives of the FPS-SESA are to study multi-scale processes and interactions that result in extreme precipitation events and to develop actionable climate information from statistical and dynamical downscaling, based on co-production with the impact and user community. To this end, different institutes contribute to this initiative that also seeks to promote inter-institutional collaboration and further networking in the South America CORDEX domain. In order to address these scientific challenges, the design of the FPS-SESA experiment assembles different purposes, namely: 1) performing ESD and RCM comparisons, 2) assessing ESD methods to simulate daily precipitation over the region, 3) assessing RCM simulations at convective permitting resolution, and 4) producing simulations as input data for crop and hydrological models to study the impact of extreme precipitation events on two main productive systems in SESA.

The present work is the first of a series of papers where the results of the FPS-SESA initiative are presented. An overview of the FPS-SESA addressing the motivations, objectives and strategies is given together with a discussion of the first results available from both RCM and ESD simulations and their comparison.

2. THE FPS-SESA EXPERIMENTAL SETUP

2.1 Data

The study of extreme precipitation requires high resolution observational data due to the discontinuous nature in time and space of these events. Even though SESA is one of the regions in South America with the highest density of precipitation records, some areas are still data sparse. For these reasons, two observational datasets are used to identify daily precipitation extremes. The daily precipitation data in the period 1979-2015 are from: (a) meteorological stations provided by the National Weather Services of Argentina, Brazil, Paraguay and Uruguay (Fig. 1 (b)); (b) the 3-hourly Multi-Source Weighted-Ensemble Precipitation (MSWEP) dataset with a 0.25° spatial resolution (Table 1, Beck et al. 2017).

Different observational precipitation datasets are also considered to assess the observational uncertainty of daily precipitation over the region (Table 1): the CPC Global dataset (CPC), the CPC morphing technique product

(CMORPH), the precipitation estimation from remotely sensed information using artificial neural networks (PERSIANN) and the Tropical Rainfall Measuring Mission dataset (TRMM).

ERA-interim reanalysis data from the European Centre for Medium-Range Weather Forecasts (Dee et al. 2011) at different spatial and time resolutions was used to force dynamic and ESD models and to evaluate the simulated daily precipitation.

2.2 Extreme precipitation events

Since FPS-SESA is focused on daily precipitation extremes, the 95th percentile of the rainy days (days with precipitation greater than or equal to 1 mm/day) in each station point or grid point is selected as a threshold for extreme precipitation considering the base period 1979-2015. Only the extended austral warm season from October to March is considered for the analysis. As depicted by the areal mean frequency of precipitation extremes across SESA, the seasons 1997-1998 and 2009-2010 show the highest occurrences of extreme precipitation events within SESA (Fig. 1 (c)). The former, with a record number of extreme precipitation events, was affected by one of the strongest El Niño events to date (Bell et al. 1999; Boulanger et al. 2005) while the latter, the warm season 2009/2010, was identified as a moderate El Niño event. Due to the larger availability of satellite-based information, the warm season 2009/2010 was selected for performing the downscaling exercises with the aim of assessing the robustness of the methods under an anomalously wet historical season. Fig. 1 (d) shows the maximum daily precipitation recorded in meteorological stations across SESA during the 2009-2010 season. The outstanding characteristics of this season are the records not only in the frequency of extreme events but also in their intensity (Fig. 1 (d)). All days within the season registered precipitation in at least one meteorological station across SESA, except for two days. The intensities of the maximum daily precipitation were also exceptional when compared with the areal 95th percentile mean of 54.1 mm/day and 99th percentile mean of 89.1 mm/day.

During the 2009-2010 warm season, three individual 3-day extreme events were chosen as case studies for analyzing specific regional processes and sensitivity to model configurations. These three extreme events were selected considering, in addition to their extreme precipitation, their spatial coverage of occurrence in at least 10% of both the meteorological stations and the MSWEP grid points in the SESA domain (Table 2, Fig. 1 (d)).

2.3 Simulation Strategies

RCM

The RCMs and institutions contributing to the FPS-SESA are shown in Table 3. The experimental design follows that of the FPS on Convective phenomena over Europe and Mediterranean (Coppola et al. 2019), where RCM simulations were performed in two modes. Weather Like (WL) mode simulations start 24 hours before the onset of each of three selected extreme events (Table 2) and run for a few days until the end of each event. As in numerical weather prediction, these simulations benefit from an accurate initial atmospheric state. Climate Mode (CM) simulations run continuously for a 6-month period starting October 1, 2009 at 00:00 UTC and ending March 31, 2010. The three extreme events occur in the CM simulations far from the initial conditions and, therefore, this simulation mode emulates typical RCM, which is a boundary value problem.

Two domains and resolutions were considered: a ~20 km horizontal grid spacing domain covering central South America (CSAM in Fig. 1a) and a ~4 km-resolution domain nested into the former focused on SESA. The SESA domain reaches the so-called convection-permitting resolution (Prein et al. 2015), where the model dynamics explicitly develops convective cells and, therefore, the deep convection parameterization was deactivated. The shallow convection parameterization was left active, though. We used two WRF (Skamarock et al. 2008) versions 3.8.1 and 3.9.1, RegCM4.7 (Coppola et al. 2019) and ETA (Mesinger et al. 2012) RCMs and a summary of the simulations setup is found in Table 3. All the models used to perform WL and CM simulations are non-hydrostatic. A one-way nesting strategy was used and no nudging technique was applied inside the domain. For ease of comparison with

observational datasets the simulations (in Mercator projections) were interpolated to the longitude-latitude grids, CSAM-20i and SESA-4i, using bilinear scheme. For 20-km simulations, 6-hourly ERA-interim reanalysis data were used as boundary and initial conditions.

ESD

Given the need to move forward with studies on the ESD methods performance to simulate the regional climate in SESA, the ESD experiment design in the framework of the FPS-SESA is twofold: to produce ESD simulations to compare with the dynamical ones (see Introduction, purpose 1) and to assess ESD methods to simulate daily precipitation over the region (see Introduction, purpose 2). Although the complete ESD experiment as well as the participating methods and evaluations will be presented in a separate paper, the present work focuses on the evaluation of some results of this experiment and the comparison with RCM results. To this end, daily precipitation from MSWEP is used as predictand in the ESD domain (Fig. 1 (a)) and ERA-Interim daily mean fields at 2° horizontal grid spacing are used as predictors. The domain considered for predictors span from 50° to 67° W and from 20° to 40°S, enclosing the SESA domain in Fig. 1 (a). The set of predictors includes circulation, moisture and temperature variables over the region: geopotential height at 500 and 1000 hPa, the meridional wind component at 850 hPa, specific humidity at 700 and 850 hPa and air temperature at 700 and 850 hPa. The choice of predictors was based on a sensitivity analysis of different sets and configurations of predictors performed in the framework of the broader ESD experiment using the daily correlation as a measure of the strength of the predictor–predictand link (Gutierrez et al. 2019) (not shown). The set of potential variables and levels of the atmosphere used as predictors was chosen based on a predictor screening performed by Bettolli and Penalba (2018) when calibrating the analog method for the southern part of SESA. The authors tested a variety of potential predictors, domains and combinations of them and found that when combined predictors of circulation variables at mid and low levels and temperature and humidity at low levels were considered, the ESD was found to be more skilful. In addition, the final predictors chosen for the ESD models analysed in the present work are representative of the synoptic environment associated with deep convection and extreme precipitation in SESA characterized by Rasmussen and Houze (2016) where a baroclinic configuration at mid to upper levels typically combines with a lee cyclone and an intensification of the Southamerican Low Level Jet, strengthening the meridional advections of humid and warm air from the Amazon to SESA. The k-folding cross-validation approach was considered to train and test ESD models, partitioning the data into 6 folds each containing 5 consecutive years. That is, fold1 covered from 1979/1980 to 1983/1984, fold2 is from 1984/1985 to 1988/1989 and so on, until fold6 from 2004/2005 to 2008/2009 warm seasons. The calibrated methods for the 1979/1980-2008/2009 period were then used to perform simulations for the independent 2009/2010 warm season. Note that this extreme precipitation season selected for RCM simulations was not included in the calibration of ESD methods in order to evaluate their robustness and to compare with RCM simulations.

Two statistical downscaling techniques are used under the perfect prognosis approach: Analogs (AN) and Generalized Linear Models (GLM). Different settings related with selection and treatment of predictors (pointwise and/or spatial-wise predictors) were considered. As the purpose of this paper is to present the comparison of RCM and ESD results in the FPS-SESA experimental framework, the simulations of only four selected ESD models participating in the ESD experiment are presented. The four ESD models and the contributing institutions are described in Table 4. The analog method (Zorita and von Storch 1999; San Martin et al. 2017; Bettolli and Penalba 2018) looks for the most similar large-scale situation (the nearest neighbour) based on Euclidean distance. The GLM consists of a two-stage implementation with Bernoulli distribution, logit link for occurrence and with Gamma distribution and log link for the amount (San Martin et al. 2017; Chandler and Wheater 2002). Atmospheric variables were considered as both spatial-wise predictors by using the principal components (PCs) explaining 95% of the total variance and pointwise predictors using the values from the four and sixteen nearest grid points to the target point for the GLM and AN, respectively (Table 4). The statistical models presented in this study broadly represent some of the most popular and widely used techniques, but still some of them have not been applied and evaluated in the region up to date (for instance, GLM techniques). Therefore, the assessment of these models in representing extremes over SESA is a contribution to the general evaluation of statistical downscaling as part of the broader ESD experiment of the FPS-SESA. The ESD methods were implemented by using the R-based climate4R open framework (Iturbide et al. 2019).

Additional dynamic simulations

Daily precipitation from the evaluation experiment in the CORDEX - South American domain available for the warm season 2009/2010 are also used for comparison purposes and to explore the sensitivity to resolution. We use CORDEX Phase I simulations from HadRM3P, RCA4, and WRF341I RCMs (Giorgi et al. 2009). Additionally, CORDEX CORE simulations from RegCM4 and REMO RCMs are also assessed (Table 1, Gutowski et al. 2016; Remedio et al. 2019). CORDEX Phase I common protocol was designed to assess regional climate downscaling and to produce large ensembles of projections based on multi-RCM simulations driven by GCM participating in CMIP5 for a set of 14 continental-scale domains. In the CORDEX-CORE framework, a standard core set of RCMs downscale a set of GCMs over all or at least most CORDEX domains for a minimum set of scenarios (Gutowski et al. 2016). CORDEX Phase I and CORDEX CORE have horizontal grid spacing, of approximately 0.44x0.44º and 0.22°x0.22º respectively. These evaluation simulations are driven by the ERA-Interim reanalysis allowing for a fair comparison with the simulations produced in the FPS-SESA initiative.

2.4 Evaluation Framework

As mentioned earlier, to carry out climate studies of spatial and temporal variability of daily precipitation extremes, it is necessary to consider as much available information as possible. For this reason, the assessment of observational uncertainty to give a reference framework against which to compare model simulations is an additional benefit. To this end, several observational datasets based on satellite, radar and in-situ observations are used in addition to meteorological stations and MSWEP dataset (Table 1). ERA Interim (ERA-I) raw precipitation data is also used as a benchmark against which the added value of downscaling can be measured.

The assessment of the different datasets and simulations (ESD and RCM) is performed using the meteorological stations (STN) as an independent reference dataset. Considering the different spatial resolutions of the datasets, the nearest grid point to each station is used for calculations. However, for illustrative purposes, some results of interpolated simulations and observations to a common grid of 0.2° using bilinear interpolation are also shown. This strategy was conducted in order to assess whether the comparison approach would influence the results.

The assessment of the different approaches focuses on the analysis of the complete warm season 2009/2010 and each 3-day extreme event selected as case-study. The skill of downscaling is evaluated following the recommendations developed within former international collaborative initiatives, VALUE-COST Action (Maraun et al. 2015) and STARDEX (Goodess et al. 2003), in order to normalize comparisons among different regions of the world. For the 2009/2010 warm season, different indices are considered to evaluate daily precipitation occurrence and amount, such as: relative frequency of wet days (R01), mean wet-day precipitation (SDII, Simple Daily Intensity Index), relative frequency of days with precipitation above 10mm (R10) and 20 mm (R20) and total precipitation amount (PRCTOT). Correlations between daily simulated and observed series considering all days (rain and non-rain days) at each station point are quantified using non-parametric Spearman correlation (ts.rs) to minimize artificial skills due to the not normally distributed precipitation. On the other hand, Pearson correlation is computed to quantify the daily correspondence in areal mean precipitation time series across SESA. Note that these metrics do not strictly assess the models' performance in reproducing the extreme precipitation itself but they are considered to evaluate the simulation of daily precipitation during the extreme precipitation season studied. As shown in Fig. 1 (b, c and d) the distinctive characteristic of this season was not only the large amounts of daily rainfall but also their frequency across SESA. Therefore, the ability of downscaling approaches in simulating the precipitation occurrence both in time and location considering different thresholds is also assessed through these metrics. Hence, they allow us to evaluate whether the models are able to capture the different aspects of the anomalously wet 2009/2010 season. In all cases, a wet day is the day that recorded precipitation $\geq$ 1 mm. Results for R01, SDII, R10 and R20 are presented as biases computed as the ratio between the simulated and the observed values.

Taylor diagrams (Taylor 2001) summarize the representation of the spatial distribution of PRCTOT and of precipitation totals for the three extreme events considered. These diagrams convey information with clarity and quantify the degree of statistical similarity between two fields (in this study, between the observed and the simulated precipitation amounts), considering the correlation coefficient, the standard deviation and the centered root mean

squared error (RMSE). In all cases, the meteorological station points within the SESA domain are used to compute the evaluation indices.

3. RESULTS

3.1 2009/2010 Warm Season

Fig. 1 (b) shows the probability associated with each observation of total precipitation during the 2009/2010 warm season considering the empirical accumulated probability function in the base period 1979-2015. High probability values (over 0.8) dominated the region, except in western Argentina. Over the central part of SESA (indicated with the rectangle in Fig. 1 (b)), the precipitation totals fell into the 99th percentile (probability values greater than 0.99), with precipitations amounts up to 1796 mm accumulated during the whole season. Taylor diagrams of PRCTOT spatial pattern are shown in Fig. 2 (a). Note that these diagrams work on centered series and, therefore, disregard model mean biases. Both observations and simulations present a large dispersion, more evident for the latter. The observational datasets (in green tones) closest to the station data correspond to MSWEP, CPC and TRMM. CMORPH and PERSIANN are far from observations, although the spatial correlations are close to 0.9, indicating that they are able to reproduce the shape of the PRCTOT field (see spatial patterns in Fig. 3). Box and whisker plots of PRCTOT considering all points within SESA show that CMORPH and PERSIANN strongly overestimate precipitation, almost doubling the observed values (Fig. 2 (b)). PRCTOT from ERA-I has a poor performance, not being able to capture neither the spatial pattern (low correlation, smaller standard deviation and high RMSE) nor the intensities (Fig. 2 and Fig. 3). Although ERA-I mean value is similar to the observed ones, the dispersion is strongly underestimated.

Overall, RCMs show a larger dispersion in their performances compared with ESD simulations; however note that ESD methods are trained to reproduce the observations (MSWEP in this case) and, therefore, this should not be straightforwardly interpreted as a better performance of ESD methods (see Casanueva et al. 2016 for further discussion on the fair intercomparison of these methods). The shape of the spatial field in SESA is relatively well captured, with correlations around 0.75, by the RegCM4 simulations in the FPS-SESA framework (RegCM4.4CM and RegCM4.20CM) as well as by ESD simulations that consider the information from local predictors (GLM_l4 and AN_l16) (Fig. 2 (a)). The former (latter) overestimate (underestimate) the spatial dispersion as depicted by the relative standard deviations larger (smaller) than 1. In terms of absolute PRCTOT, the RegCM4 simulation at convection permitting resolution (RegCM4.4CM) underestimates the observations, whereas the simulation with parameterized convection and ESD represent them reasonably well (Fig. 2 (b)). Nevertheless, the convective-permitting run performed with RegCM4 captures the spatial distribution of the accumulated precipitation during the 2009/2010 season better than the 20km run. ESD models that include spatial-wise predictor information (GLM_PC and AN_PC) and the HadRM3P follow in order of performance in representing the PRCTOT field. The remaining models exhibit spatial correlations lower than 0.6 and standard deviations with a considerable spread, but lower than the observational uncertainty associated with CMORPH and PERSIANN (Fig. 2 (a)). However, when analyzing the spatial pattern of the PRCTOT (Fig.3), most of the simulations are able to represent the spatial gradient observed with increasing values from the southwest to the northeast of the region. In some cases, such as the WRF.UCAN.20CM and WRF341I (both with parameterized convection) and RCA4, the maximum is captured but misplaced.

It is interesting to note from Fig. 3 that all CORDEX simulations and simulations from RegCM4 and WRF.UNICAN at 20km resolution show wet biases over the Andes mountains towards the west of SESA, indicating their difficulties in reproducing orographic precipitation over this complex terrain. ERA-I also show remarkable biases over that area with overestimations greater than 2700 mm during the complete warm season.

The Taylor diagram and boxplots based on interpolated simulations (Online Resource 1) do not show significant change in the daily rainfall statistics, except for the intensity of extremes in ERA-I and some RCMs, which are more intense in the interpolated fields (RegCM4.CORE, RCA4 and WRF.UCAN.20CM). This also slightly modifies the cloud of points in the Taylor diagrams, making the separation from the standard deviation smaller. From this perspective, the comparisons using either the nearest grid point or interpolations to a regular grid do not introduce any artificial skills.

The evaluation measures at daily scale are displayed in Fig. 4. Observational datasets CMORPH and PERSIANN tend to overestimate both the frequency of wet days (R01) and the wet day intensity (SDII). This overestimation also occurs to the frequency of heavy precipitation days (R20) and in the accumulated precipitation in heavy precipitation days (R20Pp, not shown), which agrees with the large overestimation in PRCTOT in Fig. 2 (b) and Fig. 3. On the other hand, despite the fact that MSWEP and CPC represent reasonably well the PRCTOT, they tend to precipitate too frequently at low intensities (large biases in R01 and SDII), whereas low biases in R20 indicate that the frequency of heavy precipitation days is well represented. TRMM performs well regarding these evaluation measures (R01, R20 and SDII). When analyzing the simulations, a large spread in the evaluation metrics is noted. ESD models tend to show similar biases to the dataset they were trained with (MSWEP), particularly the over- and under-estimation of R01 and SDII, respectively. GLM_pc and GLM_l4 additionally fail to predict the frequency of heavy precipitation events (R20). This feature of GLM models is in agreement with the documented difficulties of deterministic regression-based methods in reproducing extreme events (San Martin et al. 2017, Hertig et al 2018); note, however, that this could be alleviated by considering a stochastic version of the method (see, e.g. Gutiérrez et al. 2019). For RCM simulations, there is a noticeable spread in the evaluation measures. CORDEX simulations tend to precipitate more frequently than observed (red boxes in R01). The ability in reproducing daily intensities (SDII) depends on the model, with large underestimations of RCA4 and fairly good estimates of RegCM4.20CM, RegCM4.4CM, WRF341I and REMO.CORE. Note that the frequency of wet days (R01), which is usually overestimated by most RCMs (Solman and Blazquez, 2019) is better captured in the FPS-SESA RCM simulations performed in CM at either 20km and at convective-permitting resolution, with intensities slightly lower than observed (SDII). The exception is the RegCM4.20CM, that yields overall the best simulation of the occurrence and intensity of wet days. The number of events at higher intensities (R20) as simulated by RCM follows a similar pattern of R01, except for the CORDEX simulations WRF341I, RegCM4.CORE and REMO.CORE, that are capable of reproducing the observed values quite well, though with a moderate spatial variability. Note that given the extreme characteristics of the selected season simulated, the 20 mm threshold may not be associated with the occurrence of extreme rainfall events, at least within the 2009/2010 season.

The common shortcomings arising from the set of simulations, the systematic underestimation of the frequency and intensity of heavy rainfall events and the overestimation of the frequency of rainy days, are similar to those reported in Solman and Blazquez (2019) based on a larger set of CORDEX simulations over the South American domain. Note, however, that R01 seems to be better reproduced by the FPS simulations.

As to temporal correspondence measured by daily correlation, all RCM and ESD simulations depict similar performances, but with generally low correlation values (ts.rs in Fig. 4). As expected, regression-based ESD models show the highest correlations (around 0.5, similar to the value of MSWEP, used for training). The large spread of observational datasets is remarkable with the lowest (highest) correlations exhibited by TRMM and CPC close to that for ERA-Interim (CMORPH and PERSIAN).

ERA-I raw data has a poor performance in all evaluation metrics (Fig. 4), but particularly in reproducing the temporal agreement with observations at station point by daily correlations (ts.rs). Previous studies have found similar values in daily correlation of ERA-I for longer periods (Bettolli and Penalba, 2018), which indicates that this shortcoming of ERA-I is not exclusive of this particular 2009/2010 wet season. Most of ESD and RCM simulations analyzed here are adding value to the ERA-I since present smaller biases when compared with local observations.

Time series of areal average daily precipitations considering only the simulations of the FPS initiative are displayed in Fig. 5 (a). There is a general very good agreement between the ensemble mean of simulations and observations, indicating that both RCM and ESD models are able to reproduce the correct timing of precipitation occurrence, but not the exact location, judging from the low correlations at station points shown in Fig. 4. The spread of the RCM simulations also seems to succeed in capturing areal average precipitation intensities, whereas ESD exhibits a narrower range yielding overconfident results. In order to quantify the agreement between time series, Pearson correlations between simulations and observations were computed. Individual RCM show temporal correlations between 0.26 and 0.51, while the RCM ensemble mean reaches a correlation of 0.55. ESD models show slightly higher correlations (between 0.48 and 0.63) and the ESD ensemble mean displays a correlation of 0.59. CORDEX RCM simulations tend to be less skillful with wider spread related to considerable overestimations of areal mean precipitation (Fig.5 (b)).

Correlations values tend to be lower in agreement with these results, from 0.28 to 0.51 for individual models and 0.44 for the ensemble mean. In all cases, ensemble means outperform ERA-I and all correlations are statistically significant at the 95% confidence level after correcting by the effective sample size.

Overall, the evaluation of FPS models in reproducing precipitation features during the 2009/2010 warm season does not suggest a clear added value of the group of convective permitting simulations in comparison with the 20km and 50km simulations evaluated here, with the exception of the RegCM4.4CM experiment. Recall that the 2009/2010 season was controlled by the El Niño remote forcing, which provides the dominant large-scale circulation, a Rossby wave pattern at upper levels and an associated trough in the southeastern Pacific and an anticyclonic circulation off south Brazil that favours ascent over SESA through dynamic lift (Barreiro, 2017). This anomalous circulation favors ascending motion of warm and moist air over SESA, triggering convective systems that produce large amounts of precipitation in the region. It is worth to recall that all RCM simulations included in this analysis are driven by the ERA-Interim reanalysis, and hence, the remote forcing that exerts a dominant role during this season, is inherited through the lateral boundaries. This may explain why RCMs, independent of their setups, are capable of reproducing the main features of precipitation systems during the 2009/2010 warm season. For ESD, the different methods are also trained using large scale circulation information and, hence, allowing for capturing the dominant control of the anomalous circulation leading to anomalous rainfall. Recall also that the added value of convective permitting simulations is expected for higher moment statistics and sub-daily features of precipitation (Kendon et al. 2012), which are not tackled in this preliminary study. Note, however, that the evaluation of the sequence of events (Fig. 5), their intensity and timing allows suggesting that even at the daily scale, FPS simulations based on both RCMs and ESD yield promising results.

3.2 Extreme Precipitation Events

The extreme precipitation events selected as test cases are summarized in Table 2. The three cases are characterized by very high daily maximum precipitation intensities reaching values above 150 mm/day. The spatial extension of these events is also widespread. Case 2 is the most intense event with the largest accumulated precipitation in a day of 165.4 mm/day, but with the least areal extension as measured by the percentage of stations that accumulated more than 50 mm in the 3-day event (22%, Table 2). Conversely, in Case 1 the lowest maximum precipitation intensity of 150 mm/day is recorded in a day but the event affects a larger area (42%, Table 2). Case 3 is an intermediate situation. For brevity, Fig. 6 shows the location and spatial coverage in the different observational datasets only for Case 3. Cases 1 and 2 can be seen in Online Resource 2 and 3. Although the three events cover a large area of SESA, the regions mainly affected by heavy precipitation varies from one to another. In this regard, the ability of models to simulate the positions of individual extreme precipitation events triggered by organized deep convective systems and their areas of influence can also be assessed. An additional intention is to study their potential impacts on water resources and local agricultural systems based on the tailored data produced in the FPS-SESA framework. Case 1 covers the border between Argentina and Uruguay, affecting not only the lower Uruguay River Basin but also highly populated cities such as Buenos Aires and Montevideo (Online Resource 2). Case 2 has an elongated shape that affects the border between Argentina and Paraguay to the border between Argentina and Brazil and influences the middle Uruguay River Basin and a series of locations where soybean and maize are produced (Online Resource 3). Case 3 is a large convective system located at the border of Argentina, Brazil and Uruguay affecting some of the most productive lands in the middle to upper Uruguay River Basin (Fig. 6).

The spatial patterns of 3-days mean precipitation during the extreme events illustrated in Fig. 6 and Online Resources 2 and 3 show large disagreement among the different observational datasets in all cases. These differences are particularly noticed in the precipitation intensity, while the spatial patterns of the systems are fairly well reproduced. CMORPH and PERSIANN highly overestimate the intensity of the rainfall in agreement with the overestimation of the accumulated precipitation over the whole season studied (Fig. 3). These observational uncertainties reflect in the Taylor diagrams and box and whisker plots shown in Fig. 7. In all cases, ERA-I fails in reproducing both the intensities and locations of the events as evidenced in Fig. 6 and Fig. 7.

The performance of simulations from the CORDEX database and the FPS-SESA initiative depends on each particular case (Fig. 6 and Fig. 7 and Online Resources 2 and 3). For Case 1, the spatial correlations between all simulations and observations are lower than 0.4 (Fig. 7 (a)). When performing the evaluation using a regular grid at 0.2 resolution, correlation values tend to increase in most simulations (Online Resource 4 (a)). In this figure, WL-20 simulations (20 km resolution and with convective parameterization; yellow triangles) and GLM models (light blue circles) present correlations between 0.5 and 0.7, and climatic simulations from HadRM3P, WRF341I and RegCM4.CORE reach values even higher (between 0.65 and 0.75). Precipitation intensity distributions across SESA depicted by the box and whisker plots (Fig. 7 (b)) show that AN_pc and most CM and WL simulations perform well, though the location seems to be misplaced as depicted by RMSE values in the Taylor diagram (Fig. 7 (a)) and the simulation of spatial fields (Online Resource 3).

For Case 2, unlike the previous case, spatial correlations above 0.5 are observed for some particular models (Fig. 7 (c)) such as RegCM4 (20CM, 4CM and 4WL simulations), ETA.20WL, HadCMP3, REMO.CORE and GLM models. The skill in reproducing the spatial distribution of precipitation intensities over SESA is highly variable across simulations (Fig. 7 (d)) however with a tendency to underestimate the intensities (Fig 7 (c) and Online Resource 3). When performing the comparison using a regular grid, spatial correlations tend to decrease and the differences in box plots of intensities tend to smooth (Online Resource 4 (c) and (d)).

Case 3 seems to be the best captured from the qualitative assessment of the spatial patterns in Fig. 6. Note that this event is characterized by a small scale maximum located close to the border of Argentina, Brazil and Uruguay, with a mean intensity of around 70 mm/day, as depicted by the station data. All FPS-SESA simulations are capable of capturing the small scale features of this event, though some of the simulations misplace the maximum. However, there is a clear improvement compared with CORDEX simulations. As expected, FPS-SESA WL mode simulations generally agree better with observations than CM mode simulations. Focusing on the quantitative evaluation measures in Fig 7 (e) and (f), it is worth remarking that, similar skills among most models are observed with a tendency to underestimate the spatial variability (relative standard deviation values lower than 1) but with spatial correlations between 0.5 and 0.7, suggesting a good correspondence in the spatial distributions between simulations and observations. It is interesting to note that when comparisons are made in a regular grid (Online Resource 4 (e) and (f)), almost no changes are distinguished, indicating the robustness of simulations in this case.

As remarked above, the analysis in Fig.7 is focused on statistics based on daily precipitation, for which convective permitting simulations may not show a clear improvement compared with the 20km resolution/parameterized convection simulations. Given the extremely strong individual events occurring at very specific locations, even though they are associated with organized deep convection, it is expected that both WL-like and CM-like convective permitting simulations may misplace the location of the maxima. This behavior may explain why performance metrics summarized in Fig.7 are similar to those from CORDEX-like simulations.

4. DISCUSSION AND CONCLUSIONS

The need for understanding extreme precipitation events in SESA is increasing in the context of a remarkable increment in the frequency and intensity of these events, particularly during the late 20th century (Cavalcanti 2012; Cavalcanti et al. 2015; Carril et al., 2016). Their severe impacts on local ecosystems and socio-economic activities, as well as their projected increases in intensity in a changing climate (Giorgi et al. 2014), give rise to even greater interest. Understanding the physical mechanisms behind extreme precipitation events in SESA continues to be one of the biggest challenges. Although much work has been done to comprehend these events, identifying the factors and mechanisms that determine the location, frequency and intensity of precipitation extremes and their large impacts is not a closed matter.

This work introduces the CORDEX endorsed Flagship Pilot Study in Southeastern South America, which aims to tackle this challenge from an integrated assessment of multiple sources of observations, available climate simulations and a new set of simulations, that includes RCM experiments with resolutions from mesoscale down to convection-permitting and ESD models. The project is an inter-institutional collaborative initiative that brings together RCM and

ESD communities from different countries, as well as end-users to better support specific impact studies (agricultural and hydrological).

Preliminary results of the experiment presented here focused on the analysis of the capability of a set of downscaling methods in simulating daily precipitation during the 2009-2010 austral warm season, with particular emphasis on extreme events. The comparisons are conducted considering daily precipitation, given that ESD models contributing to this initiative are calibrated using this temporal resolution. Further analyses and intercomparisons of simulations according with different scientific aims will be presented in future papers. These will mainly be focused on assessments of the representation of the diurnal cycle of convective precipitation, where simulations at convection permitting grid spacings have demonstrated improvements when compared to coarser resolution/parameterized-convection simulations (Prein et al. 2015; Scaff et al. 2019). The analysis of the synoptic environment associated with the case studies selected and sensitivity of RCMs simulations to resolution and physics, the evaluation of ESD methods sensitivity to dataset choice and predictors choice and the study of extreme precipitation impacts on the Uruguay River Basin and on soybean and maize yields in targeted locations will also be presented in the future.

This intercomparison exercise stresses that precipitation measurement is a major challenge in SESA. Despite the growing availability of multiple observational datasets (radar, satellite, in-situ observations and combinations of them) the uncertainties are still large. Therefore, it represents one of the most important sources of uncertainty for model calibration and evaluation. No ideal gridded dataset is identified for evaluating downscaling methods from the daily precipitation perspective. CMORPH and PERSIANN tend to overestimate daily precipitation, mainly extreme values. This is in agreement with the results from Salio et al. (2015), who found that the estimates that include microwave sensors show a strong tendency to overestimate extreme precipitation over 70mm in plains such as SESA. It is worth noting that these datasets are available at high temporal resolution (hourly) and are therefore, attractive to validate sub-daily downscaling models. However, caution should be taken when analyzing precipitation amounts. MSWEP, CPC and TRMM tend to behave similarly to station data, though with some deficiencies in representing the frequency of rainy days and mean wet-day precipitation for the former and the daily correspondence for the last two datasets. Large observational uncertainties are noted in the definition of the location and intensity of extreme precipitation events. Although further analyses are needed, biases in precipitation totals might be associated with shortcomings of the algorithms used to derive precipitation amounts from infrared brightness temperature and/or the reflectivity. As discussed by Sun et al. (2018) precipitation estimates derived from satellite data show biases owing to the indirect nature of the relationship between the observations and precipitation, inadequate sampling, and deficiencies in the algorithms. Moreover, a single algorithm is not always applicable to different regions of the world therefore it should be subject to a region-dependent calibration.

Related to the observational uncertainties, the issue of evaluation of simulations against an irregular network of stations arises. A comparison between observed and simulated precipitation is a complex matter on a daily timescale due to the discontinuous nature of this variable. In this work, both RCM and ESD outputs are provided on regular grids, either because RCM provide areal-aggregated data and because ESD models are trained with the gridded MSWEP dataset. Evaluations using an irregular station network (considering the closest grid point) and a regular grid (derived from the interpolation of station data) show some changes in the models performance when using one or another, but with no clear signal of improving or worsening the models skill.

Comparisons among available climate evaluation simulations from CORDEX and the new set of RCM and ESD simulations developed in the FPS-SESA initiative reveal that there is no single model that performs best in all aspects evaluated. The ability in reproducing the different features of daily precipitation depends on the model. RCM simulations analyzed here seem to make an improvement in reproducing extreme precipitation conditions when compared with previous studies that showed that most models underpredicted extreme precipitation for month-long events over the region (Menendez et al. 2010). Moreover, some models tend to overestimate both the frequency of wet days and the frequency of extreme precipitation events. When analyzing the different simulation modes (CM and WL) and resolutions (20 and 4 km), there is no clear or systematic behavior in the results. In some cases, the CM simulations perform better than the WL simulations and in some cases simulations at convection permitting resolutions mismatch precipitation extremes.

Overall, based on the assessment of the skill of FPS RCM simulations in reproducing the precipitation behavior during the 2009/2010 warm season, including both WL and CM, parameterized convection and convection permitting experiments, there is no systematic improvement arising from the latter. Moreover, this set of simulations shows a similar skill compared with the CORDEX and CORDEX CORE simulations. Several reasons may explain this behavior. First, the 2009/2010 warm season is dominated by El Niño forcing, which exerts a strong control on the large scale circulation affecting South America and particularly SESA. This anomalous circulation favours the occurrence of rainfall events over SESA and it is demonstrated that it also favours the occurrence of extreme rainfall events (Grimm and Tedeschi, 2009). Hence, given the dominant role of the large scale forcing on rainfall, it is expected that every RCM driven by reanalysis (as it is the case in the models evaluated in this study), will inherit the main drivers leading to anomalous precipitation.

On the other hand, evaluating the mean accumulated precipitation along the entire season may not reveal any improvement arising from the higher resolution simulations. This statement may be reinforced based on the assessment of the models in reproducing the temporal evolution of the individual rainy events which show FPS-SESA simulations clearly overperforming the regular CORDEX ones. As was already discussed in the literature (Prein et al., 2015 and references therein), the added value of convective permitting simulations arise more clearly when sub daily precipitation statistics are evaluated. Though SESA is an extended region characterized by a flat terrain, convection is initiated in the Andes foothills and in the Sierras de Cordoba ranges, located in the western border of the SESA domain displayed in Fig.1 (Rasmussen and Houze, 2016) and it is propagated and upscaled further eastward. Hence, it is expected that the strongest influence of the topographic forcing arises during the early development of convective systems, which may not be reflected when evaluating daily precipitation amounts. In order to have a clearer demonstration on the advantages of convective permitting experiments, metrics based on sub daily precipitation features need to be considered. Additionally, the evaluation metrics used in this work are affected by the double-penalty, i.e. when the precipitation feature being evaluated is captured but misplaced so at each grid point the penalty of not matching the observations is accounted twice. In fact, it has been remarked throughout the analysis, mainly when evaluating the spatial distribution of the accumulated precipitation for the 2009/2010 warm season in Fig. 3 and for daily rainfall of the selected extreme events in Figs.6 and SM3, that in some cases the convective-permitting simulations outperform the coarse resolution runs, but positioning the maximum rainfall rates slightly shifted compared with observations. In these cases, performance metrics such as the RMSE or spatial correlation coefficients yield poor results being inadequate to discuss whether higher resolution improves lower resolution. Nevertheless, it is worth remarking that this work is not pursuing demonstration of the added value of convective permitting simulations per se.

ESD models tend to show an overall good performance in representing the different aspects of daily precipitation during the extreme 2009-2010 warm season. They generally exhibit similar biases to the dataset they were trained with (MSWEP), stressing the importance of the quality of the dataset chosen for calibration. As expected, deterministic statistical models tend to underestimate extreme events over the region due to they are structured to reproduce mean conditions. However, ESD models from both families (regression-based and pattern algorithms) were able to reproduce other aspects of precipitation during the anomalously wet 2009/2010 season such as PRCTOT (Fig. 2) and the timing of precipitation occurrence (Fig.5).

When focusing on individual events, it is found that most models are able to capture the extreme events selected as test cases, although with a considerable spread in accumulated daily values and the location of heavy precipitation. It is important to remark that the test cases selected in this study are characterized by very extreme conditions. Inspection of the spatial distribution of the accumulated rainfall during the 3-day events showed that, overall, ESD and RCM simulations produced in the framework of the FPS are capable of capturing the extreme conditions from rainfall events, though some of the models misplaced the maximum rainfall compared with observations. The spatial aggregation in the convective permitting simulations is remarkable when compared with lower resolution RCM. As mentioned above, inspection of sub daily precipitation statistics may help draw a clearer picture of the extent to which convective permitting simulations are useful for evaluating the impact of extreme precipitation on hydrological systems.

The poor performance of ERA-Interim raw precipitation data in all metrics and aspects evaluated is notable. From this point of view, almost all downscaling models add value in representing the different characteristics of daily precipitation over SESA.

This paper presents a synthesis of the work carried out so far in the different working groups of the FPS-SESA initiative. In this context, the basis for an engaged downscaling community and inter-institutional networking are settled. Thus, future studies will concentrate on the different purposes of the project with the ultimate goal of improving modelling of precipitation extremes over the region and generating actionable regional climate information from multiple sources.

Figure Captions

Fig. 1 (a) Region of study and domains considered for simulations: CSAM (in red) ~20 km-resolution domain covering central South America, SESA (in blue) ~4 km-resolution domain covering southeastern South America and ESD (in dark green) domain used for training and evaluation of statistical downscaling; **(b)** Spatial distribution of the meteorological stations used in this study. The probability associated with each observation of total precipitation during the 2009/2010 warm season considering the empirical accumulated probability function in the period 1979-2015 are displayed. The rectangle demarks the SESA domain; **(c)** Areal mean frequency of precipitation events that exceed the daily 95th percentile of rainy days (precipitation $\geq$ 1 mm/day) during the warm seasons over SESA. The seasons are indicated by the year of the end of the season (for instance, 1979/1980 is indicated as 1980) as depicted by the MSWEP dataset; **(d)** Maximum daily precipitation in SESA recorded in station data during the 2009/2010 warm season. Horizontal lines in the plot indicate the areal mean of the 95th and 99th percentiles (54.1 and 89.1 mm/day, respectively), while arrows indicate the three 3-day extreme precipitation events selected as case-study.

Fig. 2 (a) Taylor diagram of PRCTOT during the 2009/2010 warm season using the closest grid point to each meteorological station. Standard deviation and centred root mean square errors are normalized by the observed standard deviation. Each point in the Taylor diagram represents an observational dataset or a model; **(b)** Box and whisker plots of PRCTOT across all grid points closest to station points over SESA. On each box, the central mark indicates the median, and the bottom and top edges of the box indicate the 25th and 75th percentiles, respectively. The whiskers extend to the 5th and 95th percentiles and the points indicate the maximum observed or simulated PRCTOT value in SESA. Station data in black, green tones correspond to observations, yellow tones to 20km FPS-SESA RCM simulations, purple tones to 4km FPS-SESA RCM simulations, red tones to CORDEX RCM simulations and blue tones to ESD simulations.

Fig. 3 Total precipitation amount (PRCTOT) during the 2009/2010 warm season for the set of observations, CORDEX-RCM simulations, FPS-SESA ESD and RCM simulations performed in climate mode at 20 km (20CM) and at 4 km (4CM).

Fig. 4 Box and whisker plots of performance indices for the set of observations, CORDEX-RCM simulations and FPS-SESA ESD and RCM simulations during the 2009/2010 warm season across SESA. The indices were computed using the closest grid point to the station point. R01, R20 and SDII are relative biases (ratio between simulated and observed values). ts.rs: daily Spearman correlation. On each box, the central mark indicates the median, and the bottom and top edges of the box indicate the 25th and 75th percentiles, respectively. The whiskers extend to the most extreme data points.

Fig. 5 Daily areal mean precipitation time series over SESA as depicted by the observations at station points, the ensemble of RCM simulations from FPS-SESA and ensemble of ESD simulations (solid lines) **(a)** and the ensemble of RCM simulations from CORDEX and ERA-I (solid lines) **(b)**. The shading indicates the range of the ensemble

members in each case. Pearson correlation values of observed temporal series and each individual model and ensemble means are indicated.

Fig. 6 Daily mean precipitation during Case 3: 21 to 23-11-2009 for the set of observations, CORDEX-RCM simulations, FPS-SESA ESD and RCM simulations performed in climate mode and weather like mode at 20km (20CM and 20WL) and at 4km (4CM and 4WL).

Fig. 7 Taylor diagrams of daily mean precipitation during each test case using the closest grid point to each meteorological station. Standard deviation and centred root mean square errors are normalized by the observed standard deviation. Case1: 19 to 21-02-2010 ((a) and (b)), Case 2: 18 to 20-01-2010 ((c) and (d)) and Case 3:21 to 23-11-2009 ((e) and (f)).

Table Captions

Table 1 Gridded precipitation datasets used in this study.

Table 2 Description of the three case-studies selected.

Table 3 RCM and contributing institutions to the FPS-SESA.

Table 4 ESD methods used in this study and contributing institutions to the FPS-SESA.

References

Ashouri H, Hsu KL, Sorooshian S, Braithwaite DK, Knapp KR, Cecil LD, Prat OP (2015) PERSIANN-CDR: Daily precipitation climate data record from multi-satellite observations for hydrological and climate studies. Bulletin of the American Meteorological Society 96: 69–83. https://doi.org/10.1175/BAMS-D-13-00068.1

Barreiro M (2010) Influence of ENSO and the south Atlantic ocean on climate predictability over Southeastern South America. Clim. Dyn. 35: 1493-1508. https://doi.org/10.1007/s00382-009-0666-9

Barreiro M (2017) Interannual variability of extratropical transient wave activity and its influence on rainfall over Uruguay.Int. J. Climatol. DOI: 10.1002/joc.5082

Barros V, Clarke R, Silva Dias PL (2006) Climate change in the La Plata Basin, CIMA-CONICET, 1ra ed., Buenos Aires

Barros VR and Doyle ME (2018) Low-level circulation and precipitation simulated by CMIP5 GCMS over southeastern South America. International Journal of Climatology 38: 5476–5490. https://doi.org/10.1002/joc.5740

Beck HE, van Dijk AIJM, Levizzani V, Schellekens J, Miralles DG, Martens B, de Roo A (2017) MSWEP: 3-hourly 0.25° global gridded precipitation (1979–2015) by merging gauge, satellite, and reanalysis data, Hydrology and Earth System Sciences Discussions. https://doi.org/10.5194/hess-21-589-2017

Bell GD, Halpert MS, Ropelewski CF, Kousky VE, Douglas AV, Schnell RC, Gelman ME (1999) Climate Assessment for 1998. BAMS. https://doi.org/10.1175/1520-0477-80.5s.S1

Bettolli ML, Penalba OC (2014) Synoptic sea level pressure patterns–daily rainfall relationship over the Argentine Pampas in a multi-model simulation. Meteorol. Appl. 21: 376–383. https://doi.org/10.1002/met.13

Bettolli ML, Penalba OC (2018) Statistical downscaling of daily precipitation and temperatures in southern La Plata Basin. International Journal of Climatology 38: 3705–3722. https://doi.org/10.1002/joc.5531

Boulanger JP, Leloup J, Penalba O, Rusticucci M, Lafon F, Vargas W (2005) Observed precipitation in the Paraná-Plata hydrological basin: long-term trends, extreme conditions and ENSO teleconnections. Clim Dyn 24: 393-413. https://doi.org/10.1007/s00382-004-0514-x

Carril, AF, Iracema FA Cavalcanti, CG Menendez, A Sörensson, N López-Franca, JA Rivera, F Robledo, PG Zaninelli, T Ambrizzi, OC Penalba, RP da Rocha, E Sánchez, ML Bettolli, N Pessacg, M Renom, R Ruscica, S Solman, B Tencer, AM Grimm, M Rusticucci, ACherchi, R Tedeschi, L Zamboni (2016).Extreme events in the La Plata basin: a retrospective analysis of what we have learned during CLARIS-LPB project. Clim Res, 68 (2-3): 95-116.

Cavalcanti IFA (2012) Large scale and synoptic features associated with extreme precipitation over South America: a review and case studies for the first decade of the 21st century. Atmos. Res. 118: 27–40. http://dx.doi.org/10.1016/j.atmosres.2012.06.012

Cavalcanti, I.F.A., A.F. Carril, O.C. Penalba, A.M. Grimm, C.G. Menéndez, E. Sanchez, A. Cherchi, A. Sörensson, F. Robledo, J. Rivera, V. Pántano, M.L. Bettolli, P. Zaninelli, L. Zamboni, R.G. Tedeschi, M. Dominguez, R. Ruscica, h, R. Flach. 2015. Precipitation extremes over La Plata Basin – Review and new results from observations and climate simulations. Journal of Hydrology. Volume 523, April 2015, Pages 211–230. doi:10.1016/j.jhydrol.2015.01.028

Casanueva A, Herrera S, Fernández J, Gutiérrez JM (2016) Towards a fair comparison of statistical and dynamical downscaling in the framework of the EURO-CORDEX initiative. Climatic change 137(3-4): 411-426. https://doi.org/10.1007/s10584-016-1683-4

Chandler RE, Wheater HS (2002) Analysis of rainfall variability using generalized linear models: A case study from the west of Ireland. Water Resour. Res. 38: 1192. https://doi.org/10.1029/2001WR000906

Coppola E, Sobolowski S, Pichelli E, Raffaele F, Ahrens B, Anders I, Ban N, Bastin S, Belda M, Belusic D, Caldas‐Alvarez A, Cardoso RM, Davolio S, Dobler A, Fernandez J, Fita L, Fumiere Q, Giorgi F, Goergen K, Güttler I, Halenka T, Heinzeller D, Hodnebrog O, Jacob D, Kartsios S, Katragkou E, Kendon E, Khodayar S, Kunstmann H, Knist S, Lavín‐Gullón A, Lind P, Lorenz T, Maraun D, Marelle L, van Meijgaard E, Milovac J, Myhre G, Panitz H-J, Piazza M, Raffa M, Raub T, Rockel B, Schär C, Sieck K, Soares PMM, Somot S, Srnec L, Stocchi P, Tölle MH, Truhetz H, Vautard R, de Vries H, Warrach‐Sagi K (2019) A first-of-its-kind multi-model convection permitting ensemble for investigating convective phenomena over Europe and the Mediterranean. Clim. Dyn. https://doi.org/10.1007/s00382-018-4521-8

da Rocha RP, Morales CA, Cuadra SV, Ambrizzi T (2009) Precipitation diurnal cycle and summer climatology assessment over South America:an evaluation of Regional Climate Model version 3 simulations. J Geophys Res 114. D10108. https://doi.org/10.1029/2008JD010212

Dee DP, Uppala SM, Simmons AJ, Berrisford P, Poli P, Kobayashi S, Andrae U, Balmaseda MA, Balsamo G, Bauer P, Bechtold P, Beljaars ACM, van de Berg L, Bidlot J, Bormann N, Delsol C, Dragani R, Fuentes M, Geer AJ, Haimberger L, Healy SB, Hersbach H, Hólm EV, Isaksen L, Kållberg P, Köhler M, Matricardi M, McNally AP, Monge-Sanz BM, Morcrette JJ, Park BK, Peubey C, de Rosnay P, Tavolato C, Thépaut JN, Vitart F (2011) The ERA-Interim reanalysis: configuration and performance of the data assimilation system, Q. J. Roy. Meteorol. Soc. 137: 553–597. https://doi.org/10.1002/qj.828

D'onofrio A, Boulanger JP, Segura EC (2010) CHAC: a weather pattern classification system for regional climate downscaling of daily precipitation. Climatic Change 98: 405–427. https://doi.org/10.1007/s10584-009-9738-4

Doyle ME, Barros VR (2002) Midsummer low-level circulation and precipitation in subtropical South America and related sea surface temperature anomalies in the South Atlantic. J. Climate 15: 3394–3410. https://doi.org/10.1175/1520-0442(2002)015<3394:MLLCAP>2.0.CO;2

Durkee JD, Mote TL, Shepherd M (2009) The contribution of mesoscale convective complexes to rainfall across subtropical South America. J. Climate 22: 4590–4605. https://doi.org/10.1175/2009JCLI2858.1

Falco M, Carril AF, Menéndez CG, Zaninelli PG, Li LZ (2019) Assessment of CORDEX simulations over South America: added value on seasonal climatology and resolution considerations. Climate Dynamics 52: 4771–4786. https://doi.org/10.1007/s00382-018-4412-z

Fowler HJ, Blenkinsop S, Tebaldi C (2007) Linking climate change modelling to impacts studies: recent advances in downscaling techniques for hydrological modelling. International Journal of Climatology 27: 1547-1578. https://doi.org/10.1002/joc.1556

Giorgi F, Jones C, Asrar G (2009) Addressing climate information needs at the regional level: the CORDEX framework. WMO Bulletin, 58, 175–183.

Giorgi F, Coppola E, Raffaele F, Tefera Diro G, Fuentes-Franco R, Giuliani G, Mamgain A, Llopart M, Mariotti L, Tormaand C (2014) Changes in extremes and hydroclimatic regimes in the CREMA ensemble projections. Climatic Change 125: 39–51. https://doi.org/10.1007/s10584-014-1117-0

Grimm AM, Tedeschi RG (2009) ENSO and Extreme Rainfall Events in South America. Journal of Climate 22: 1589–1609. doi:10.1175/2008jcli2429.1

Gutiérrez JM, Maraun D, Widmann M, Huth R, Hertig E, Benestad R, Roessler O et al (2019) An Intercomparison of a Large Ensemble of Statistical Downscaling Methods over Europe: Results from the VALUE Perfect Predictor Cross-Validation Experiment. International Journal of Climatology 39 (9): 3750-85. https://doi.org/10.1002/joc.5462

Goodess CM, Haylock MR, Jones PD, Bardossy A, Frei C, Schmith T (2003) Statistical and Regional dynamical Downscaling of Extremes for European regions: some preliminary results from the STARDEX project 2003EGS-AGU-EUG Joint Assembly, Nice, 6-11 April Geophysical Research Abstracts, vol. 5. http://www.cosis.net/abstracts/EAE03/02934/EAE03-J02934.pdf

Gutowski JW, Giorgi F, Timbal B, Frigon A, Jacob D, Kang HS, Raghavan K, Lee B, Lennard C, Nikulin G et al (2016) WCRP COordinated Regional Downscaling EXperiment (CORDEX): A diagnostic MIP for CMIP6. Geosci. Model Dev. 9: 4087–4095. https://doi.org/10.5194/gmd-9-4087-2016

Haylock MR, Cawley GC, Harpham C, Wilby RL and Goodess CM (2006), Downscaling heavy precipitation over the United Kingdom: a comparison of dynamical and statistical methods and their future scenarios. Int. J. Climatol. 26: 1397-1415. https://doi.org/10.1002/joc.1318

Hertig E, Maraun D, Bartholy J, Pongracz R, Vrac M, Mares I, Gutiérrez JM, Wibig J, Casanueva A, Soares PMM (2018) Comparison of statistical downscaling methods with respect to extreme events over Europe: Validation results from the perfect predictor experiment of the COST Action VALUE. Int. J. Climatol 39: 3846– 3867. https://doi.org/10.1002/joc.5469

Huffman GJ, Bolvin DT, Nelkin EJ, Wolff DB, Adler RF, Gu G et al (2007) The TRMM Multisatellite Precipitation Analysis (TMPA): Quasi-global, multiyear, combined-sensor precipitation estimates at fine scales. J. Hydrometeor. 8: 38–55. https://doi.org/10.1175/JHM560.1

Huth R, Mikšovský J, Štěpánek P, Belda M, Farda A, Chládová Z, Pišoft P (2015) Comparative validation of statistical and dynamical downscaling models on a dense grid in central Europe: temperature. Theoretical and applied climatology 120(3-4): 533-553. https://doi.org/10.1007/s00704-014-1190-3

Iturbide M, Bedia J, Herrera S, Baño-Medina J, Fernández J, Frías MD, Manzanas R, San-Martín D, Cimadevilla E, Cofiño AS, Gutiérrez JM (2019) The R-based climate4R open framework for reproducible climate data access and post-processing. Environmental Modelling and Software 111: 42–54. https://doi.org/10.1016/j.envsoft.2018.09.009

Jacob D, Elizalde A, Haensler A, Hagemann S, Kumar P, Podzun R, Rechid D, Remedio AR, Saeed F, Sieck K, Teichmann C, Wilhelm C (2012) Assessing the Transferability of the regional climate model REMO to different

coordinated regional climate downscaling experiment (CORDEX) regions. Atmosphere 3(4): 181–199. https://doi.org/10.3390/atmos3010181

Jones RG, Noguer M, Hassell D, Hudson D, Wilson S, Jenkins G, Mitchell J (2003) Workbook on gen-erating high resolution climate change scenarios using PRECIS. Met Office Hadley Centre Rep., pp 32

Joyce RJ, Janowiak JE, Arkin PA, Xie P (2004) CMORPH: A method that produces global precipitation estimates from passive microwave and infrared data at high spatial and temporal resolution. J. Hydrometeor 5: 487–503, https://doi.org/10.1175/1525-7541(2004)005<0487:CAMTPG>2.0.CO;2

Kendon EJ, Roberts NM, Senior CA, Roberts MJ (2012) Realism of rainfall in a very high resolution regional climate model. J. Climate, 25, 5791–5806, doi:10.1175/JCLI-D-11-00562.1

Kupiainen M, Jansson C, Samuelsson P, Jones C (2014) Rossby Centre regional atmospheric model, RCA4. Rossby Center News Letter

Llopart M, Coppola E, Giorgi F, da Rocha RP, Cuadra SV (2014) Climate change impact on precipitation for the Amazon and La Plata basins. Climatic change 125: 111-125. https://doi.org/10.1007/s10584-014-1140-1

Maraun D, Wetterhall F, Ireson AM, Chandler RE, Kendon EJ, Widmann M, Brienen S, Rust HW, Sauter T, Themeßl M, Venema VKC, Chun KP, Goodess CM, Jones RG, Onof C, Vrac M, Thiele-Eich I (2010) Precipitation downscaling under climate change. Recent developments to bridge the gap between dynamical models and the end user. Reviews of Geophysics 48: 1–34, RG3003. https://doi.org/10.1029/2009RG000314

Maraun D, Widmann M, Gutierrez JM, Kotlarski S, Chandler RE, Hertig E, Wibig J, Huth R, Wilcke RAI (2015) VALUE - A Framework to Validate Downscaling Approaches for Climate Change Studies. Earth's Future 3(1): 1-14. https://doi.org/10.1002/2014EF000259

Menéndez CG, de Castro M, Boulanger JP et al (2010) Downscaling extreme month-long anomalies in southern South America, Climatic Change 98: 379. https://doi.org/10.1007/s10584-009-9739-3

Mesinger F, Chou SC, Gomes JL, Jovic D, Bastos P, Bustamante JF, Lazic L, Lyra A, Morelli S, Ristic I, Veljovic K (2012) An upgraded version of the Eta model. Meteorol Atmos Phys, 116:63-79

Nesbitt S, Cifelli R, Rutledge S (2006) Storm morphology and rainfall characteristics of TRMM precipitation features. Mon. Weather. Rev. 134: 2702–2721. https://doi.org/10.1175/MWR3200.1

Prein AF, Langhans W, Fosser G, Ferrone A, Ban N, Goergen K, Keller M, Tölle M, Gutjahr O, Feser F et al (2015) A review on regional convection- permitting climate modeling: Demonstrations, prospects, and challenges, Rev. Geophys. 53: 323– 361. https://doi.org/10.1002/2014RG000475

Rasmussen KL, Houze RA Jr (2016) Convective initiation near the Andes in subtropical South America. Mon. Wea. Rev.144: 2351-2374

Reboita MS, Dutra LMM, Dias CG (2016) Diurnal cycle of precipitation simulated by RegCM4 over South America: present and future scenarios. Clim. Res. 70: 39-55. https://doi.org/10.3354/cr01416

Remedio AR, Teichmann C, Buntemeyer L, Sieck K, Weber T, Rechid D, Hoffmann P, Nam C, Kotova L, Jacob D (2019) Evaluation of New CORDEX Simulations Using an Updated Köeppen–Trewartha Climate Classification. Atmosphere 10: 726. https://doi.org/10.3390/atmos10110726

Rummukainen M (2010) State-of-the-art with regional climate models. WIREs Climate Change 1: 82–96. https://doi.org/10.1002/wcc.8

Rozante JR, Cavalcanti IFA (2008) Regional Eta model experiments: SALLJEX and MCS development. J. Geophys. Res. 113, D17106. http://dx.doi.org/10.1029/2007JD009566

Salio P, Nicolini M, Zipser EJ (2007) Mesoscale convective systems over Southeastern South America and their relationship with the South American low level jet. Mon. Weather Rev. 135: 1290–1309. https://doi.org/10.1175/MWR3305.1

Salio P, Hobouchian MP, García Skabar Y, Vila D (2015) Evaluation of high-resolution satellite precipitation estimates over southern South America using a dense rain gauge network. Atmospheric Research 163: 146-161.

San Martín D, Manzanas R, Brands S, Herrera S, Gutiérrez JM (2017) Reassessing model uncertainty for regional projections of precipitation with an ensemble of statistical downscaling methods. Journal of Climate 30: 203–223. https://doi.org/10.1175/JCLI-D-16-0366.1

Saulo CA, Seluchi M, Nicolini M (2004) A case study of a Chaco low-level jet event. Mon. Wea. Rev. 132: 2669–2683. https://doi.org/10.1175/MWR2815.1

Scaff L, Prein AF, Li Y, Liu C, Rasmussen R, Ikeda K (2019) Simulating the convective precipitation diurnal cycle in North America's current and future climate. Climate Dynamics https://doi.org/10.1007/s00382-019-04754-9

Seluchi ME, Marengo JA (2000) Tropical–mid latitude exchange of air masses during summer and winter in South America: Climatic aspects and examples of intense events. International Journal of Climatology 20: 1167–1190. https://doi.org/10.1002/1097-0088(200008)20:10<1167::AID-JOC526>3.0.CO;2-T

Skamarock W, Klemp J, Dudhia J, Gill D, Barker D, Duda M, Wang W, Powers J (2008) A description of the advanced research WRF version 3 (No. NCAR/TN-475+STR) . University Corporation for Atmospheric Research. http://dx.doi.org/10.5065/D68S4MVH

Solman SA and Blázquez J (2019) Multiscale precipitation variability over South America: Analysis of the added value of CORDEX RCM simulations. Clim Dyn. 53: 1547-1565. https://doi.org/10.1007/s00382-019-04689-1

Sun Q et al., 2018. A review of global precipitation data sets: data sources, estimation, and intercomparisons. Review of Geophysics, 56, 79-107

Taylor KE (2001) Summarizing multiple aspects of model performance in a single diagram, J. Geophys. Res., 106(D7), 7183– 7192. https://doi.org/10.1029/2000JD900719

Teixeira MS, Satyamurty P (2007) Dynamical and synoptic characteristics of heavy rainfall episodes in Southern Brazil. Mon. Weather Rev. 135: 598–617. https://doi.org/10.1175/MWR3302.1

Ungerovich M, Barreiro M (2019) Dynamics of extreme rainfall events in summer in southern Uruguay. Int. J. Climatol. 39: 3655-3667. https://doi.org/10.1002/joc.6046

Xie P, Chen M, Shi W (2010) CPC global unified gauge-based analysis of daily precipitation, Preprints, 24th Conf. on Hydrology, Atlanta, GA, Amer. Meteor. Soc 2

Zorita E. and von Storch H (1999) The analog method as a simple statistical downscaling technique: comparison with more complicated methods. Journal of Climate 12: 2474–2489. https://doi.org/10.1175/1520-0442

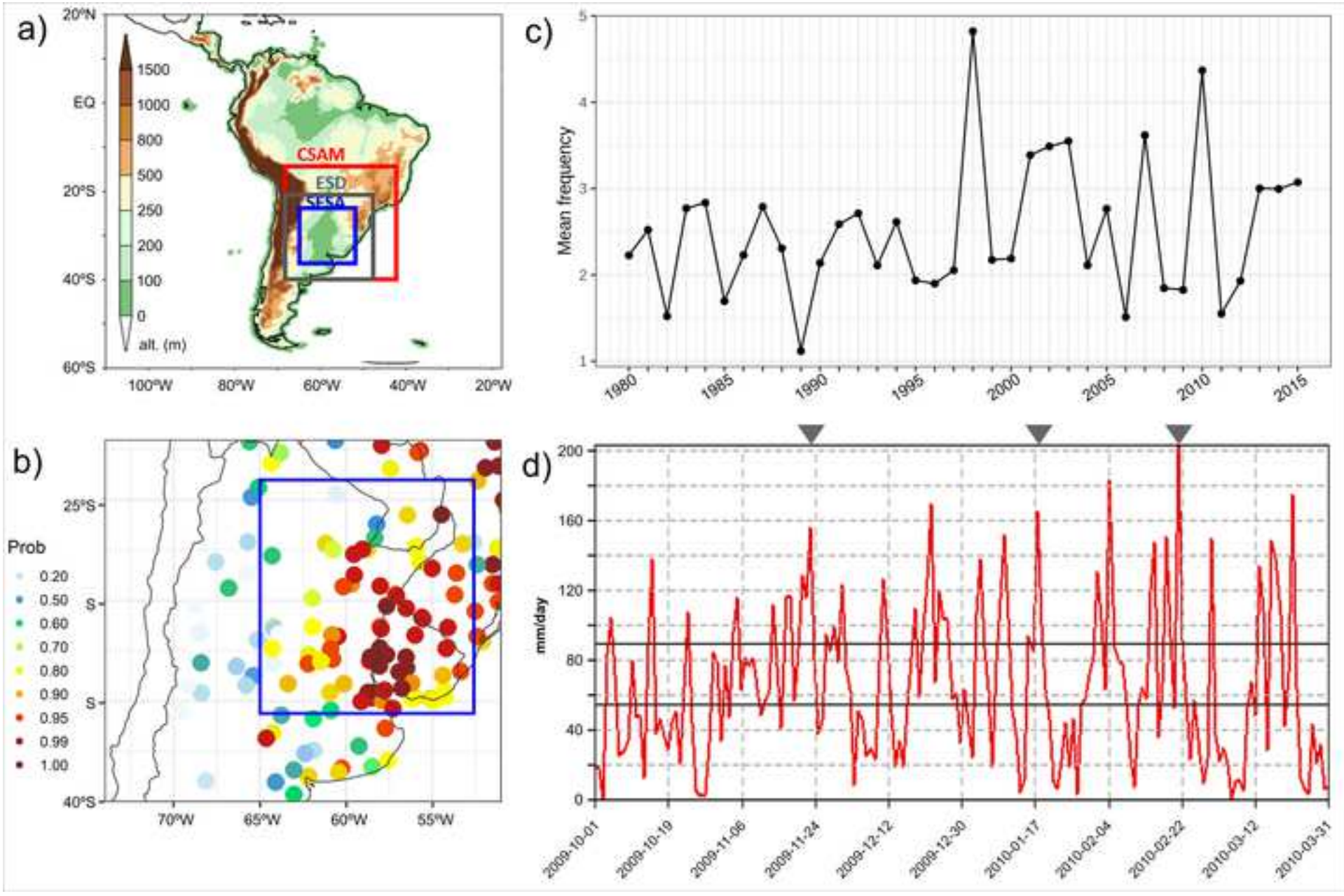
a)
20°N
EQ
20°S
40°S
60°S
100°W
80°W
60°W
40°W
20°W
1500
1000
800
500
250
200
100
0
alt. (m)
CSAM
ESD
SESA
c)
Mean frequency
1
2
3
4
5
1980
1985
1990
1995
2000
2005
2010
2015
b)
Prob
0.20
0.50
0.60
0.70
0.80
0.90
0.95
0.99
1.00
25°S
S
S
40°S
70°W
65°W
60°W
55°W
d)
mm/day
0
40
80
120
160
200
2009-10-01
2009-10-19
2009-11-06
2009-11-24
2009-12-12
2009-12-30
2010-01-17
2010-02-04
2010-02-22
2010-03-12
2010-03-31

Fig. 1

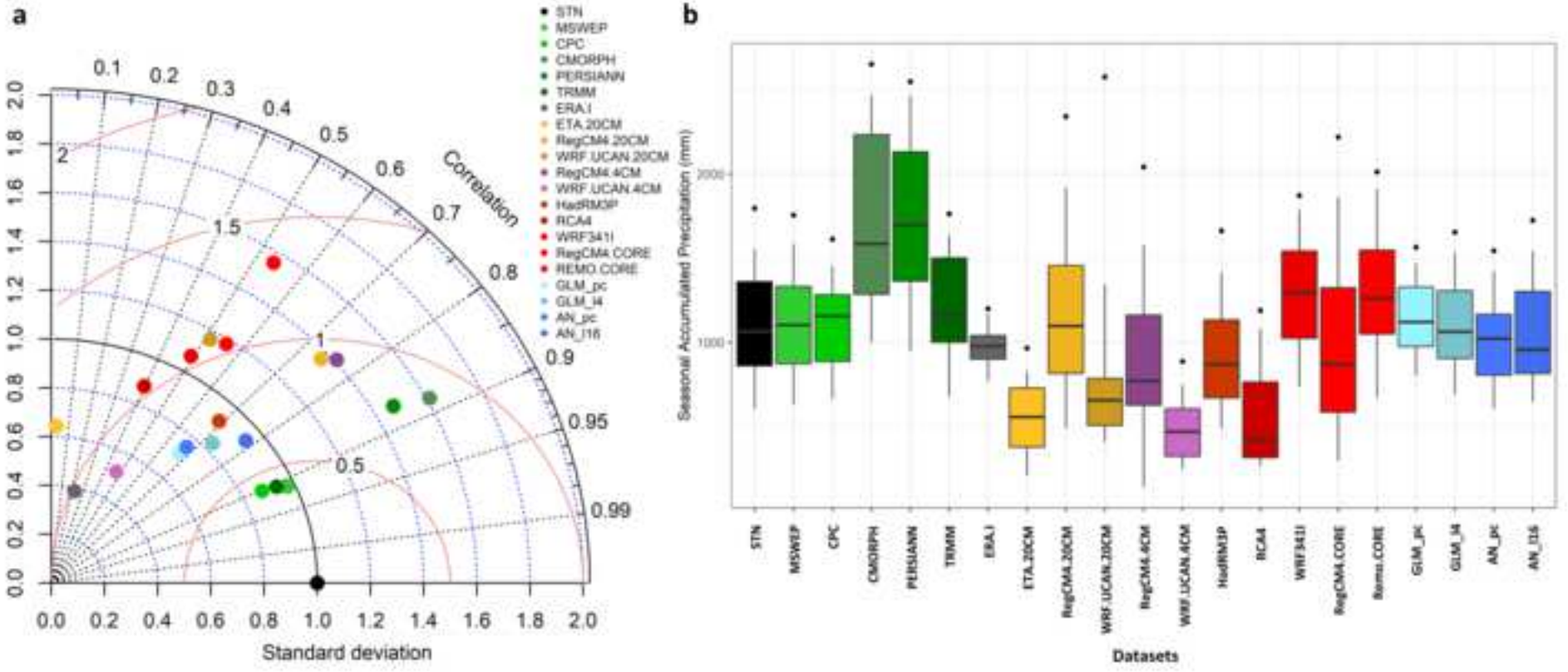
a
b
STN
MSWEP
CPC
CMORPH
PERSIANN
TRMM
ERA.I
ETA.20CM
RegCM4.20CM
WRF.UCAN.20CM
RegCM4.4CM
WRF.UCAN.4CM
HadRM3P
RCA4
WRF341I
RegCM4.CORE
REMO.CORE
GLM_pc
GLM_I4
AN_pc
AN_I16
Correlation
Standard deviation
Seasonal Accumulated Precipitation (mm)
Datasets

Fig. 2

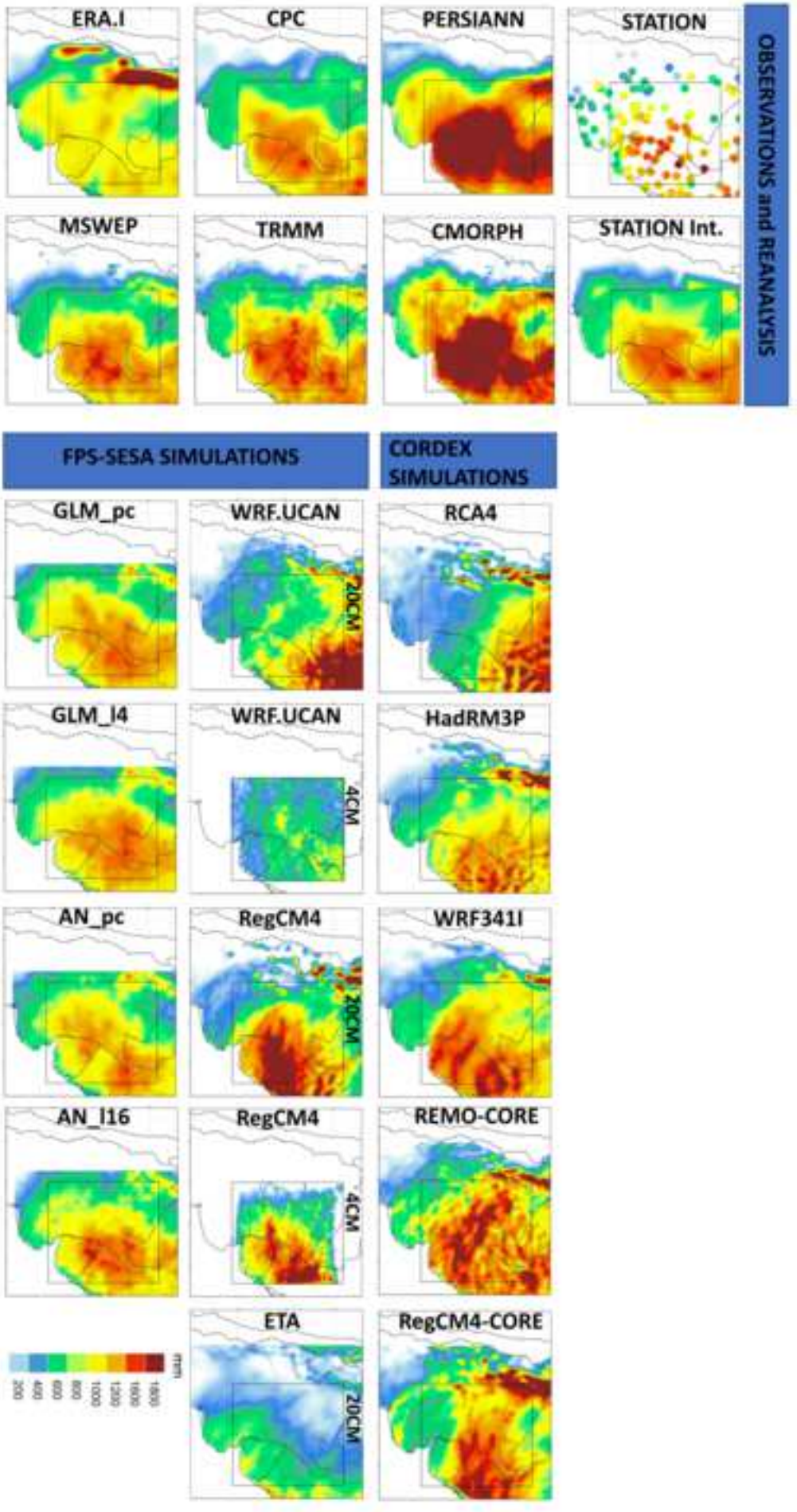
ERA.I
CPC
PERSIANN
STATION
OBSERVATIONS and REANALYSIS
MSWEP
TRMM
CMORPH
STATION Int.
FPS-SESA SIMULATIONS
CORDEX SIMULATIONS
GLM_pc
WRF.UCAN
20CM
RCA4
GLM_l4
WRF.UCAN
4CM
HadRM3P
AN_pc
RegCM4
20CM
WRF341I
AN_l16
RegCM4
4CM
REMO-CORE
ETA
20CM
RegCM4-CORE
mm
200
400
600
800
1000
1200
1400
1600

Fig. 3

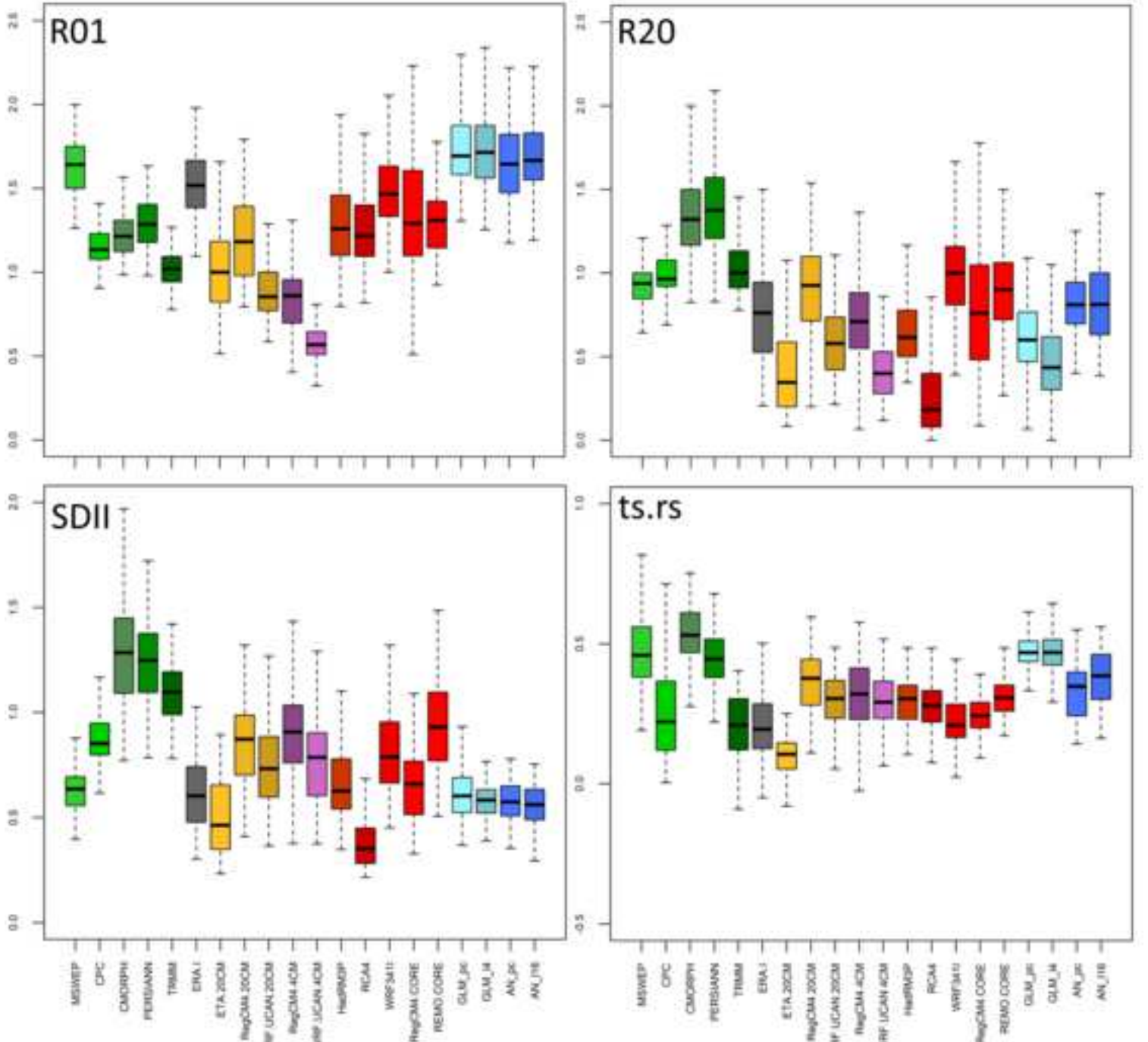
R01
R20
SDII
ts.rs
MSWEP
CPC
CMORPH
PERSIANN
TRMM
ERA.I
ETA.20CM
RegCM4.20CM
WRF.UCAN.20CM
RegCM4.4CM
WRF.UCAN.4CM
HadRM3P
RCA4
WRF3411
RegCM4.CORE
REMO.CORE
GLM_jpl
GLM_l4
AN_jpl
AN_l18

Fig. 4

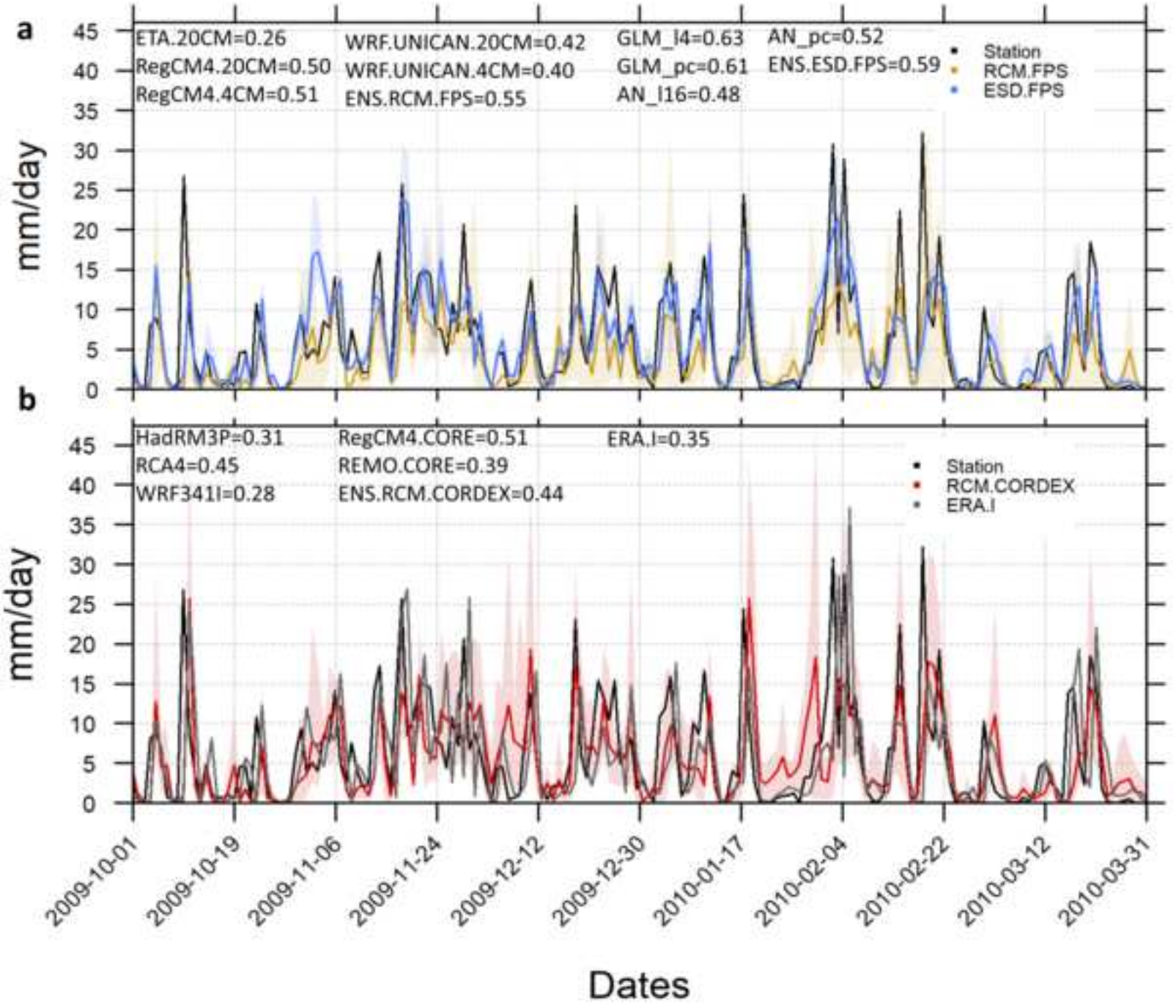
a
ETA.20CM=0.26
RegCM4.20CM=0.50
RegCM4.4CM=0.51
WRF.UNICAN.20CM=0.42
WRF.UNICAN.4CM=0.40
ENS.RCM.FPS=0.55
GLM_I4=0.63
GLM_pc=0.61
AN_I16=0.48
AN_pc=0.52
ENS.ESD.FPS=0.59
Station
RCM.FPS
ESD.FPS
mm/day
b
HadRM3P=0.31
RCA4=0.45
WRF341I=0.28
RegCM4.CORE=0.51
REMO.CORE=0.39
ENS.RCM.CORDEX=0.44
ERA.I=0.35
Station
RCM.CORDEX
ERA.I
mm/day
2009-10-01
2009-10-19
2009-11-06
2009-11-24
2009-12-12
2009-12-30
2010-01-17
2010-02-04
2010-02-22
2010-03-12
2010-03-31
Dates

Fig. 5

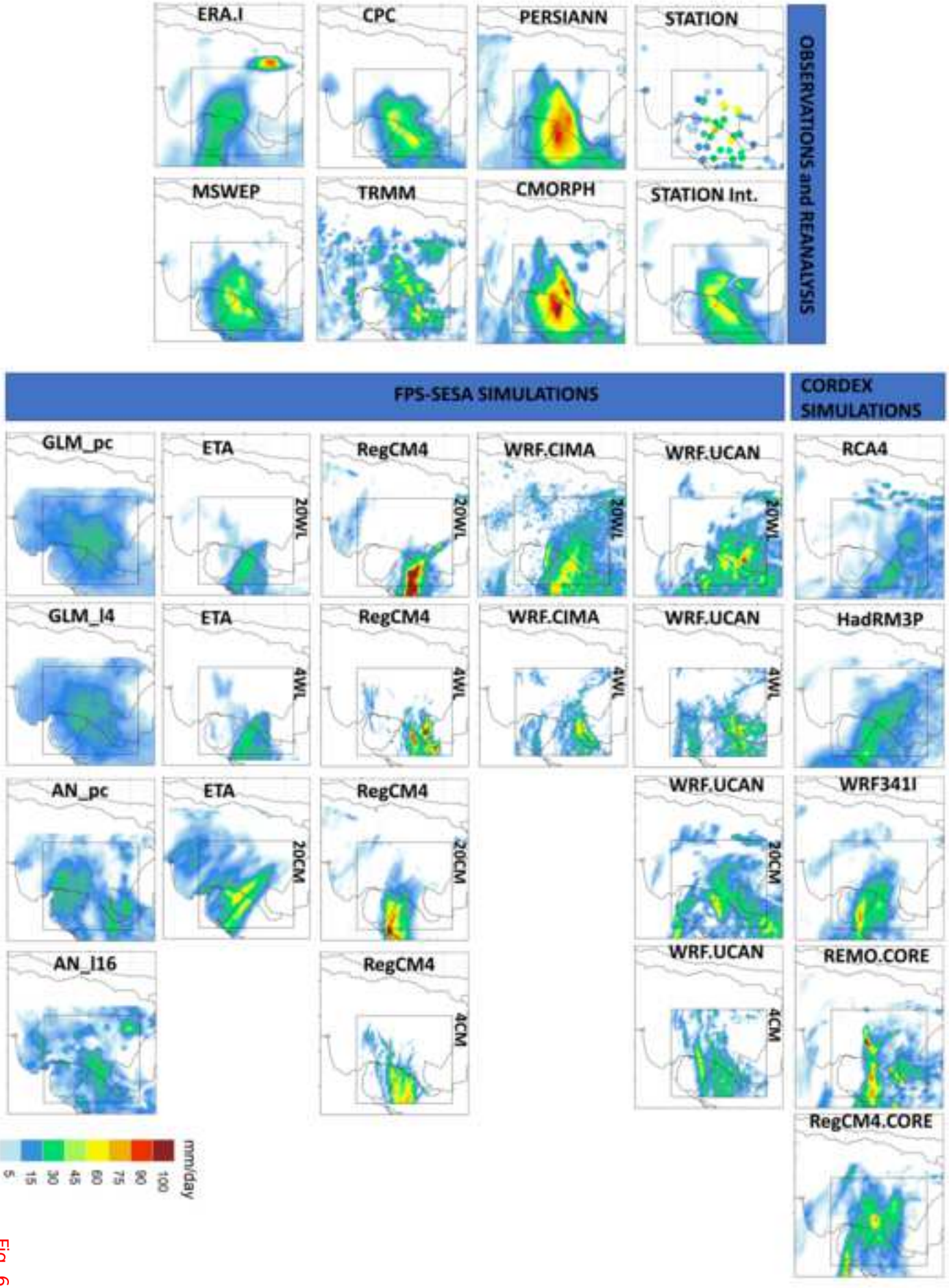
ERA.I
CPC
PERSIANN
STATION
OBSERVATIONS and REANALYSIS
MSWEP
TRMM
CMORPH
STATION Int.
FPS-SESA SIMULATIONS
CORDEX SIMULATIONS
GLM_pc
ETA
20WL
RegCM4
20WL
WRF.CIMA
20WL
WRF.UCAN
20WL
RCA4
GLM_l4
ETA
4WL
RegCM4
4WL
WRF.CIMA
4WL
WRF.UCAN
4WL
HadRM3P
AN_pc
ETA
20CM
RegCM4
20CM
WRF.UCAN
20CM
WRF341I
AN_l16
RegCM4
4CM
WRF.UCAN
4CM
REMO.CORE
RegCM4.CORE
5
15
30
45
60
75
90
100
mm/day

Fig. 6

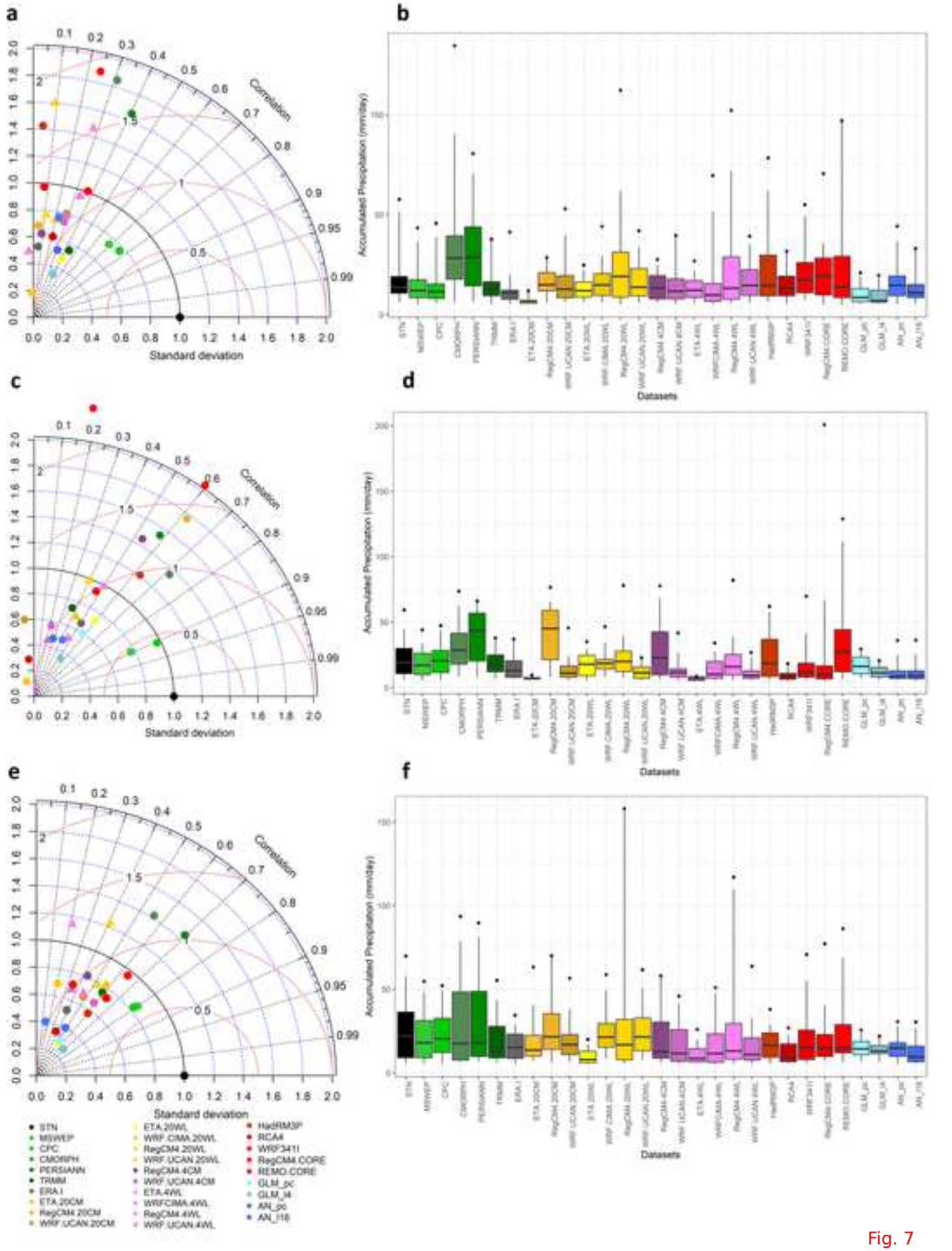
a
b
c
d
e
f
Correlation
Standard deviation
Accumulated Precipitation (mm/day)
Datasets
STN
MSWEP
CPC
CMORPH
PERSIANN
TRMM
ERA.I
ETA.20CM
RegCM4.20CM
WRF.UCAN.20CM
ETA.20WL
WRF.CIMA.20WL
RegCM4.20WL
WRF.UCAN.20WL
RegCM4.4CM
WRF.UCAN.4CM
ETA.4WL
WRFCIMA.4WL
RegCM4.4WL
WRF.UCAN.4WL
HadRM3P
RCA4
WRF341I
RegCM4.CORE
REMO.CORE
GLM_pc
GLM_t4
AN_pc
AN_I16

Fig. 7

Table 1 Gridded precipitation datasets used in this study.

	Dataset	Label	Grid Resolution	Reference
Observational Datasets	MSWEP	MSWEP	0.25°	Beck et al. 2017
	CPC-Global	CPC	0.5°	Xie et al. 2010
	CMORPH	CMORPH	0.25°	Joyce et al. 2004
	PERSIANN-CDR	PERSIANN	0.25°	Ashouri et al. 2015
	TRMM 3B42	TRMM	0.25°	Huffman et al. 2007
	Stations Interpolation	STN	0.2º	
CORDEX-RCM	HadRM3P	HadRM3P	0.44°	Jones et al. 2003
	RCA4	RCA4	0.44°	Kupiainen et al. 2014
	WRF	WRF341I	0.44°	Skaramock et al. 2008
	REMO	REMO.CORE	0.22°	Jacob et al. 2012
	RegCM4	RegCM4.CORE	0.22°	Giorgi et al. 2012
Reanalysis	ERA-Interim	ERA-I	0.75°	Dee et al. 2011

Table 2 Description of the three case-studies selected.

Event	3-day Event	Initialization Procedure (WL)	Maximum Daily Precipitation during the event	Percentage of Stations with 3-day Accumulated Precipitation>50mm
Case 1	19-02-2010 to 21-02-2010	Start: 18-02-2010 00:00 UTC End: 22-02-2010 00:00 UTC	150 mm/day	42%
Case 2	18-01-2010 to 20-01-2010	Start: 17-01-2010 00:00 UTC End: 20-01-2010 00:00 UTC	165.4 mm/day	22%
Case 3	21-11-2009 to 23-11-2009	Start: 20-11-2009 00:00 UTC End: 23-11-2009 00:00 UTC	155.5 mm/day	31%

Table 3 RCM and contributing institutions to the FPS-SESA.

RCM	Label (model name+spatial resolution+type of simulation)	Status of simulations	Institution
RegCM4	RegCM4.4WL	Finished	University of Sao Paulo - São Paulo State University
	RegCM4.20WL	Finished	
	RegCM4.4CM	Finished	
	RegCM4.20CM	Finished	
ETA	ETA.4WL	Finished	National Institute for Space Research-Brazil
	ETA.20WL	Finished	
	ETA.4CM	In progress	
	ETA.20CM	Finished	
WRF381	WRF.UCAN.4WL	Finished	University of Cantabria/CSIC
	WRF.UCAN.20WL	Finished	
	WRF.UCAN.4CM	Finished	
	WRF.UCAN.20CM	Finished	
WRF391	WRF.CIMA.4WL	Finished	CIMA-University of Buenos Aires-CONICET
	WRF.CIMA.20WL	Finished	
	WRF.CIMA.4CM	In progress	
	WRF.CIMA.20CM	In progress	

Table 4 ESD methods used in this study and contributing institutions to the FPS-SESA

Family	Label	Configuration	Institution
Generalized Linear Models	GLM_pc	PCs of all predictor variables (95% variance)	University of Cantabria/CSIC University of Buenos Aires/CONICET
	GLM_l4	Local predictor values in the four nearest grid boxes.	
Analogs	AN_pc	Nearest neighbor. PCs of all predictor variables (95% variance)	University of Cantabria/CSIC University of Buenos Aires/CONICET
	AN_l16	Nearest neighbor. Local predictor values in the sixteen nearest grid boxes.	